

Determination of S_{17} from ${}^8\text{B}$ breakup by means of the method of continuum-discretized coupled-channels

K. Ogata,¹ S. Hashimoto,¹ Y. Iseri,² M. Kamimura,¹ and M. Yahiro¹

¹*Department of Physics, Kyushu University, Fukuoka 812-8581, Japan*

²*Department of Physics, Chiba-Keizai College, Todoroki-cho 4-3-30, Inage, Chiba 263-0021, Japan*

(Dated: December 28, 2018)

The astrophysical factor for ${}^7\text{Be}(p, \gamma){}^8\text{B}$ at zero energy, $S_{17}(0)$, is determined from ${}^{208}\text{Pb}({}^8\text{B}, p+{}^7\text{Be}){}^{208}\text{Pb}$ at 52 MeV/nucleon. We use the method of continuum-discretized coupled-channels (CDCC) to accurately calculate the ${}^8\text{B}$ breakup cross section, taking account of nuclear breakup, Coulomb dipole and quadrupole transitions and higher-order processes. The asymptotic normalization coefficient (ANC) method is used to extract $S_{17}(0)$ from the calculated breakup-cross-section. The main result of the present paper is $S_{17}(0) = 21.4_{-1.9}^{+2.0}$ eV b. This result has +4.5%/−2.6% theoretical error, which comes from ambiguity of the p - ${}^7\text{Be}$ scattering length, and 8.4% systematic experimental error. CDCC calculation with one-step Coulomb dipole transitions results in a smaller value of $S_{17}(0)$, 20.2 eV b, which is almost consistent with the extracted value with the first-order perturbation theory: 18.9 eV b. Inclusion of Coulomb quadrupole transitions in one-step CDCC calculation is found to give further reduction of $S_{17}(0)$, i.e. 18.8 eV b. Multistep processes give about 12% contribution to $S_{17}(0)$ in the present case. The analysis with the ANC method is also applied to direct measurement of ${}^7\text{Be}(p, \gamma){}^8\text{B}$ and $S_{17}(0) = 22.2_{-0.58}^{+0.68}$ eV b is obtained, which agrees very well with the result of precise measurement of the p -capture reaction: $S_{17}(0) = 22.1 \pm 0.6$ (expt) ± 0.6 (theo) eV b. Thus, the discrepancy between the values of $S_{17}(0)$ obtained from direct ${}^7\text{Be}(p, \gamma){}^8\text{B}$ and indirect ${}^8\text{B}$ -breakup measurements is essentially removed.

PACS numbers: 24.10.Eq, 25.60.Gc, 25.70.De, 26.65.+t

I. INTRODUCTION

The solar neutrino problem is one of central issues in the neutrino physics [1]. The current interpretation of the solar-neutrino deficit is the neutrino oscillation induced by the mass difference among ν_e , ν_μ and ν_τ , and their mixing angles [2], then attention is now focused on determining the oscillation parameters with observations. The astrophysical factor S_{17} , defined by $S_{17}(E) = \sigma_{p\gamma}(E)E \exp[2\pi\eta]$ with $\sigma_{p\gamma}$ the cross section of the p -capture reaction ${}^7\text{Be}(p, \gamma){}^8\text{B}$ and η the Sommerfeld parameter, plays an essential role in the solar-neutrino oscillation phenomenology, in the sense that the prediction value for the flux of ${}^8\text{B}$ neutrino, which is intensively detected on the earth, is proportional to the zero-incident-energy limit of $S_{17}(E)$, i.e. $S_{17}(0)$. The required accuracy for $S_{17}(0)$ from astrophysics is about 5% in errors [3].

Recently, precise measurement of $\sigma_{p\gamma}(E)$, i.e. $S_{17}(E)$, has been carried out by Junghans *et al.* [4] at energies of $E = 116\text{--}2460$ keV, which are rather small but still higher than stellar energies (~ 20 keV), and $S_{17}(0) = 22.1 \pm 0.6$ (expt) ± 0.6 (theo) eV b was derived by extrapolating the measured $S_{17}(E)$ with a three-cluster model [5] for ${}^8\text{B}$ structure. However, this extrapolation is still ambiguous, since the three-cluster model does not reproduce the measured $S_{17}(E)$ sufficiently in both magnitude and E -dependence. Actually, as pointed out in Ref. [6], uncertainty of the p - ${}^7\text{Be}$ scattering length (about 50% in error) prevents one from determining $S_{17}(0)$ with very high accuracy.

Because of difficulties of the direct measurement at

stellar energies, alternative indirect measurements were proposed. Coulomb dissociation [7, 8, 9, 10, 11, 12, 13] of ${}^8\text{B}$ is one of such indirect measurements. So far extraction of $S_{17}(0)$ from these experiments was based on the virtual photon theory, which assumes that the ${}^8\text{B}$ is dissociated through its one-step Coulomb dipole (E1) transitions, i.e., with no multistep E1 transitions, no nuclear breakup and no Coulomb quadrupole (E2) transitions. In the analysis of MSU experiment [12, 13], exceptionally, the E2 contribution, estimated from the parallel-momentum-distribution of ${}^7\text{Be}$ fragment, was reduced from the breakup spectrum of ${}^8\text{B}$. As a result, the extracted $S_{17}(0)$ is $17.8_{-1.2}^{+1.4}$ eV b, which is somewhat smaller than that obtained from RIKEN experiment, $S_{17}(0) = 18.9 \pm 1.8$ eV b [9]. However, the recent experiment done at GSI [11] showed that the E2 contribution is negligibly small, i.e. the measured cross section can be interpreted as a result of breakup process corresponding to the E1 transitions. The resulting $S_{17}(0)$ is $18.6 \pm 1.2 \pm 1.0$ eV b. Thus, roles of the E2 component are still under discussion. More seriously, there exists a non-negligible discrepancy of about 15% between the values of $S_{17}(0)$ derived from direct p -capture and indirect ${}^8\text{B}$ -breakup measurements.

Very recently, it was shown by semiclassical calculation of ${}^{208}\text{Pb}({}^8\text{B}, p+{}^7\text{Be}){}^{208}\text{Pb}$ at 52 MeV/nucleon, the RIKEN beam energy, that the discrepancy mentioned above was significantly reduced by the inclusion of nuclear-breakup components, E2 transitions and higher-order processes [14]. Motivated by this result, in the present paper we attempt to extract a reliable value of $S_{17}(0)$ from ${}^8\text{B}$ dissociation experiment measured at

RIKEN [7, 8, 9], with a sophisticated method with three-body reaction model, that is, the method of continuum-discretized coupled-channels [15, 16] (CDCC). CDCC was shown to describe various processes where effects of projectile-breakup are essential [17, 18, 19, 20, 21, 22, 23, 24, 25], and it has also been applied to ^8B nuclear and Coulomb breakup with high degrees of success [13, 26, 27, 28].

In order to extract $S_{17}(0)$ from the result of the CDCC analysis of ^8B breakup based on the $p+^7\text{Be}+\text{A}$ three-body model, we use the asymptotic normalization coefficient (ANC) method [29, 30], which accurately determines $S_{17}(0)$ if the tail of the ^8B wave function, described by the Whittaker function times the ANC, is well determined. As important advantage of the use of the ANC method, the reaction mechanism is not restricted; namely, nuclear breakup, E2 transitions and higher-order processes can all be included. Additionally, the error of $S_{17}(0)$ coming from the use of the ANC method can quantitatively be evaluated, as mentioned in Refs. [25, 28]. Actually, it was shown in Ref. [28] that $S_{17}(0)$ can be determined by CDCC and the ANC method from ^8B breakup even at 3.2 MeV/nucleon, where nuclear breakup and higher-order processes are essentially important.

It was found, however, that the 3.2 MeV/nucleon data [31] contain an irrelevant component to $S_{17}(0)$, which corresponds to the $1/2^-$ ^7Be excited-state in the final channel; this $1/2^-$ ^7Be component is shown to have a contribution of order 10% to the ground state of ^8B [32]. Therefore, the evaluated value of $S_{17}(0)$ in Ref. [28], 22.3 ± 0.64 (theo) ± 2.23 (expt) eV b, should be assumed as an upper limit of $S_{17}(0)$. The irrelevant component was removed in RIKEN, GSI and MSU experiments, by detecting the emitted ^7Be in its ground state. However, the $1/2^-$ ^7Be excited-state may play a dynamical role during breakup processes of ^8B . In other words, description of ^8B breakup beyond the three-body model, say, the $p+^3\text{He}+^4\text{He}+\text{A}$ four-body model illustrated in Fig. 1, may be required to determine S_{17} with high accuracy. Thus, one needs justification of the use of a reaction model based on the $p+^7\text{Be}+\text{A}$ three-body model instead of the $p+^3\text{He}+^4\text{He}+\text{A}$ four-body model.

The purpose of the present paper is as follows. First, we theoretically estimate four-body dynamical effects on ^8B breakup cross sections and show the validity of the three-body CDCC analysis of ^8B dissociation. Second, we determine S_{17} from $^{208}\text{Pb}(^8\text{B}, p+^7\text{Be})^{208}\text{Pb}$ at 52 MeV/nucleon by the ANC method, taking account of nuclear and Coulomb breakup and all higher-order processes. It should be noted that in our CDCC calculation interference between nuclear- and Coulomb-breakup amplitudes is explicitly included. In numerical calculation we make use of the eikonal-CDCC method (E-CDCC) [33], with some modifications, to obtain the scattering amplitude corresponding to large values of the orbital-angular-momentum L between the projectile and the target nucleus. We then construct a hybrid am-

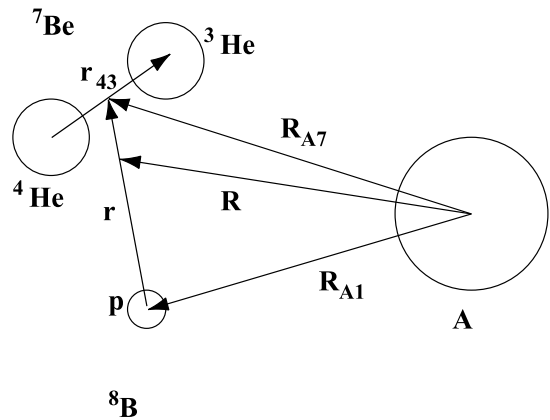


FIG. 1: Illustration of the $p+^3\text{He}+^4\text{He}+\text{A}$ four-body system. Here A is a target.

plitude from the results of E-CDCC and CDCC. This method allows one to make very accurate analysis of nuclear and Coulomb breakup of ^8B with high computational speed [33]. Uncertainties of the extracted $S_{17}(0)$ from the ^8B breakup by means of CDCC and the ANC method are carefully evaluated. Finally, we discuss the extracted value of $S_{17}(0)$ from the viewpoint of contributions of E2 transitions and higher-order processes. The ANC method is also applied to direct $^7\text{Be}(p, \gamma)^8\text{B}$ measurement and the difference between the values of $S_{17}(0)$ derived from direct and indirect measurements is evaluated.

In Sec. II A the ANC method is briefly reviewed and in Sec. II B we describe ^8B breakup on the basis of the $p+^3\text{He}+^4\text{He}+\text{A}$ four-body model and show that it can be reduced to the $p+^7\text{Be}+\text{A}$ three-body model. Formulation of modified E-CDCC and construction of the hybrid scattering amplitude are described in Sec. II C. We analyze in Sec. III A the ^8B breakup cross section measured at RIKEN with CDCC and extract $S_{17}(0)$ by the ANC method. In Sec. III B uncertainties of the extracted $S_{17}(0)$ and effects of the intrinsic spin of ^8B are quantitatively evaluated. Effects of resonance states of ^8B on the breakup cross section are discussed in Sec. III C. The value of the extracted $S_{17}(0)$ is then discussed and compared with that obtained by the virtual photon theory in Sec. III D. Roles of E2 transitions and higher-order processes are also discussed and the ANC method is applied to precise direct measurement of $^7\text{Be}(p, \gamma)^8\text{B}$. Final summary and conclusions are given in Sec. IV.

II. FORMALISM

A. The ANC method

Let us consider the radiative capture reaction $p+^7\text{Be} \rightarrow ^8\text{B} + \gamma$ in the low incident-energy limit. The reaction

is then dominated by the Coulomb dipole (E1) transitions and is quite peripheral, since the E1 operator suppresses a contribution of the inner part of the ${}^8\text{B}$ wave function to the cross section $\sigma_{p\gamma}(E)$. The reaction is thus determined only by the tail of the ${}^8\text{B}$ wave function in the ground state, $\phi_8^{(0)}$. Outside the range R_N of nuclear force working between p and ${}^7\text{Be}$, which turned out to be about 4 fm, the radial part of $\phi_8^{(0)}$ with respect to \mathbf{r} has a simple form, i.e.

$$\varphi_8^{(0)}(r) \approx CW_{-\eta, \ell+1/2}(2k_0r)/r, \quad r > R_N, \quad (1)$$

where k_0 is the relative wave-number between p and ${}^7\text{Be}$ and $W_{-\eta, \ell+1/2}$ is the Whittaker function with ℓ the orbital angular momentum between p and ${}^7\text{Be}$ in the ground state of ${}^8\text{B}$, i.e. $\ell = 1$ in the present case. The constant C in Eq. (1) is precisely the ANC we focus on. One can find that the cross section $\sigma_{p\gamma}(0)$, or $S_{17}(0)$, is proportional to C^2 , by taking the matrix elements of E1 transitions with the use of Eq. (1). Xu *et al.* [30] found that the proportionality constant $S_{17}(0)/C^2$ is $1/0.026$. In the present paper we take account of small but non-negligible dependence of $S_{17}(0)/C^2$ on scattering wave-functions between p and ${}^7\text{Be}$ used in analysis. Following Baye [34], we use the formula

$$S_{17}(0) \approx 38.0(1 - 0.0013\bar{a}_s)C^2, \quad (2)$$

where \bar{a}_s is the p - ${}^7\text{Be}$ scattering length.

It is possible to determine the ANC from similar reactions involving virtual or real breakup of ${}^8\text{B}$, if the reaction is peripheral, namely, the inner part of the ${}^8\text{B}$ wave function has no contribution. When experimental data are available on such a reaction, the ANC is given by the relation between the experimental and theoretical cross sections,

$$\mathfrak{S}_{\text{exp}} \equiv \frac{\sigma_{\text{exp}}}{\sigma_{\text{calc}}} = \frac{C^2}{\alpha^2}. \quad (3)$$

In theoretical calculation, the unknown wave function of ${}^8\text{B}$ is replaced by a single-particle wave function with a known constant α , i.e. the single-particle ANC. Hence, we can extract $S_{17}(0)$ from the spectroscopic factor $\mathfrak{S}_{\text{exp}}$ determined from indirect measurements. It should be noted that $\mathfrak{S}_{\text{exp}}$ thus obtained has quite strong dependence on the choice of the ${}^8\text{B}$ wave function. In fact, the ANC method is not suitable for deriving physically-meaningful $\mathfrak{S}_{\text{exp}}$, since $\mathfrak{S}_{\text{exp}}$ contains all information of the inner part of the ${}^8\text{B}$ wave function. On the contrary, the ANC C in Eq. (3) is a physical quantity if the reaction concerned is peripheral, thus it should be determined uniquely. As shown in Sec. III B, $\mathfrak{S}_{\text{exp}}$ and α depend on the single-particle wave function taken, but C hardly depends on it. Consequently, a cross section at extremely low energies can indirectly determined with high accuracy; this prescription is called the ANC method [29].

The ANC method thus designed was originally proposed for p -transfer reactions and actually applied

to ${}^{10}\text{Be}({}^7\text{Be}, {}^8\text{B}){}^9\text{Be}$ [35], ${}^{14}\text{N}({}^7\text{Be}, {}^8\text{B}){}^{13}\text{C}$ [36], and ${}^7\text{Be}(d, n){}^8\text{B}$ [25]. In the present paper, alternatively, we aim to extract the ANC from ${}^8\text{B}$ dissociation by ${}^{208}\text{Pb}$ target at intermediate energies. For forward-scattering of ${}^8\text{B}$, the dissociation process is obviously peripheral with respect to R defined in Fig. 1, from the viewpoint of the classical trajectory. However, peripherality concerned with r , which is an essential condition required by the ANC method, is not obvious and needs be examined. When the Coulomb force is expanded in terms of multipoles, E1 operator becomes dominant at large R . The operator is, up to a constant,

$$\frac{R}{(wr)^2}\theta(wr - R) + \frac{wr}{R^2}\theta(R - wr), \quad (4)$$

where $w = 7/8$ ($w = 1/8$) for the Coulomb force between A and p (${}^7\text{Be}$). As mentioned above, the trajectory of ${}^8\text{B}$ corresponding to forward scattering belongs to large values of R , say $R \geq R_{\text{min}}$. In the first term of Eq. (4), large R corresponds to large r , i.e. $r \geq R_{\text{min}}/w$. Thus the tail region of the ${}^8\text{B}$ wave function contributes to the E1 transitions. In the second term, conversely, large R corresponds to small r , i.e. $0 \leq r \leq R_{\text{min}}/w$; however, the small r region is not important because of the factor r/R^2 in front of the theta function. Thus, the insensitivity of the ${}^8\text{B}$ breakup cross section at forward angles to the inner part of the ${}^8\text{B}$ wave function is shown to be true also for Coulomb breakup. Quantitative estimation of this insensitivity is done in Sec. III B.

B. Extraction of ANC from ${}^8\text{B}$ breakup

So far, CDCC analysis of ${}^8\text{B}$ Coulomb dissociation [13, 26, 27, 28] was based on the $p+{}^7\text{Be}+A$ three-body model, namely the three-body CDCC was used. However, as mentioned in Sec. I, it is not obvious whether ${}^7\text{Be}$ behaves as an inert particle in the reaction, since the energy of the first-excited state of ${}^7\text{Be}$ is quite small, i.e. 0.4291 MeV. Moreover, ${}^7\text{Be}$ has rather small separation-energy, $E_s = 1.5866$ MeV, relative to the lowest ${}^3\text{He}+{}^4\text{He}$ threshold. Hence, we should consider as a more reliable model the $p+{}^3\text{He}+{}^4\text{He}+A$ four-body model illustrated in Fig. 1. We then start with the model and show that it can be reduced, with some reasonable approximations, to the $p+{}^7\text{Be}+A$ three-body model.

Let us consider A as a heavy target just for simplicity. The triple differential cross section for $({}^8\text{B}, {}^7\text{Be}+p)$ reaction is obtained by $\mathcal{C}\rho|\mathfrak{T}|^2$ with a given factor \mathcal{C} and the three-body phase space factor ρ [37]. The transition amplitude for ${}^8\text{B}$ breakup is

$$\mathfrak{T} = \langle \chi_1 \chi_7 \phi_7^{(0)} | U_{A3} + U_{A4} + U_{A1} + V_{13} + V_{14} | \Psi_{4\text{-body}} \rangle, \quad (5)$$

where χ_1 (χ_7) is the plane wave of outgoing p (${}^7\text{Be}$) relative to A, $\phi_7^{(0)}$ the ground state of ${}^7\text{Be}$, and $\Psi_{4\text{-body}}$ the total (four-body) wave function in the initial channel. Here, U_{XY} (V_{XY}) is the optical potential (two-body

interaction) between two nuclei X and Y and the subscripts 1, 3, 4 and A represent p , ${}^3\text{He}$, ${}^4\text{He}$ and A, respectively. Since the main part of $U_{A3} + U_{A4}$, which includes the nuclear and Coulomb interactions, is the central force, one can expand it in terms of multipoles: $U^{(\lambda)}[Y_\lambda(\hat{\mathbf{r}}_{43}) \otimes Y_\lambda(\hat{\mathbf{R}}_{A7})]_{00}$, where λ denotes the multipolarity. The coupling $U'_{A7} \equiv \langle \phi_7^{(1)} | U_{A3} + U_{A4} | \phi_7^{(0)} \rangle$ between the $p_{3/2}$ ground-state of ${}^7\text{Be}$, $\phi_7^{(0)}$, and its $p_{1/2}$ first-excited-state, $\phi_7^{(1)}$, is much smaller than the single-folding potential $U_{A7} \equiv \langle \phi_7^{(0)} | U_{A3} + U_{A4} | \phi_7^{(0)} \rangle$, since the dominant $\lambda = 0$ component of the multipoles contributes to U_{A7} but not to U'_{A7} . The same statement is possible for coupling to other highly-excited-states of ${}^7\text{Be}$, not only for discrete states but also continuum ones. However, as an exception, coupling between the ground state and a scattering state of ${}^3\text{He}$ - ${}^4\text{He}$ with $s_7 = 3/2$, where s_7 is the total spin of ${}^7\text{Be}$, contains the $\lambda = 0$ component. Furthermore, Coulomb dipole ($\lambda = 1$) transitions of ${}^7\text{Be}$ may play a role in the ${}^8\text{B}$ dissociation process. Fortunately, it is confirmed by ${}^3\text{He}+{}^4\text{He}+{}^{208}\text{Pb}$ three-body model calculation that ${}^7\text{Be}$ breakup cross sections at intermediate energies are less than about 1% of the elastic cross section for $\theta_7 \lesssim 4^\circ$, where θ_7 is the scattering angle of the c.m. of ${}^7\text{Be}$. Thus, ${}^7\text{Be}$ can be assumed to be inert in the breakup process of ${}^8\text{B}$ as long as θ_7 is small. In general θ_7 can differ from the ${}^8\text{B}$ scattering angle θ_8 in the ${}^8\text{B} \rightarrow p+{}^7\text{Be}$ process. However, the difference between θ_7 and θ_8 is very small, since the energy transfer of the ${}^8\text{B}$ breakup reaction concerned here is much smaller than the incident energy of ${}^8\text{B}$. In actual ANC analysis, as one sees below, we use experimental data at very forward angles of θ_8 . Thus, one can regard ${}^7\text{Be}$ as an inert particle in calculation of the breakup cross section of ${}^8\text{B}$.

We are then able to replace $U_{A3} + U_{A4}$ by U_{A7} in \mathfrak{T} . Similarly, $V_{13} + V_{14}$ can be replaced by the corresponding single-folding potential $V_{17} \equiv \langle \phi_7^{(0)} | V_{13} + V_{14} | \phi_7^{(0)} \rangle$. As a result of the replacement, \mathfrak{T} contains the overlap

$$\begin{aligned} \langle \phi_7^{(0)} | \Psi_{4\text{-body}} \rangle &= \langle \phi_7^{(0)} | \frac{i\varepsilon}{E - H_{4\text{-body}} + i\varepsilon} | \phi_8^{(0)} e^{i\mathbf{P}\cdot\mathbf{R}} \rangle \\ &\approx \frac{i\varepsilon}{E - e_7 - H_{3\text{-body}} + i\varepsilon} | \mathfrak{S}_{\text{exp}}^{1/2} \psi_{17}(\mathbf{r}) e^{i\mathbf{P}\cdot\mathbf{R}} \rangle, \end{aligned} \quad (6)$$

where \mathbf{P} is the momentum conjugate to \mathbf{R} and $H_{4\text{-body}}$ represents the Hamiltonian of the four-body system. In Eq. (6) $\mathfrak{S}_{\text{exp}}^{1/2} \psi_{17}(\mathbf{r}) \equiv \langle \phi_7^{(0)}(\mathbf{r}_{43}) | \phi_8^{(0)}(\mathbf{r}_{43}, \mathbf{r}) \rangle$; namely, $\psi_{17}(\mathbf{r})$ stands for the normalized wave function between ${}^7\text{Be}$ and p in ${}^8\text{B}$, where both ${}^7\text{Be}$ and ${}^8\text{B}$ are in the ground states. The spectroscopic factor $\mathfrak{S}_{\text{exp}}$ means the incompleteness of the two-body ($p+{}^7\text{Be}$) picture for $\phi_8^{(0)}$. Moreover, e_7 is the eigenenergy of $\phi_7^{(0)}$ and $H_{3\text{-body}}$ is the three-body Hamiltonian defined by

$$H_{3\text{-body}} = T_r + T_R + V_{17}(\mathbf{r}) + U_{A7}(\mathbf{R}_{A7}) + U_{A1}(\mathbf{R}_{A1}), \quad (7)$$

where T_r and T_R show the kinetic-energy operators concerned with \mathbf{r} and \mathbf{R} , respectively. Inserting the approx-

imate form of $\langle \phi_7^{(0)} | \Phi_{4\text{-body}} \rangle$ into Eq. (5) leads to

$$\begin{aligned} \mathfrak{T} &\approx \mathfrak{S}_{\text{exp}}^{1/2} \mathfrak{T}_{3\text{-body}}, \\ \mathfrak{T}_{3\text{-body}} &\equiv \langle \chi_1 \chi_7 \phi_7^{(0)} | U_{A7} + U_{A1} + V_{17} | \Psi_{3\text{-body}} \rangle, \end{aligned} \quad (8)$$

where the three-body wave function $\Psi_{3\text{-body}}$ is a solution of the Schrödinger equation $(H_{3\text{-body}} + e_7 - E) | \Psi_{3\text{-body}} \rangle = 0$. Here E is the total energy of the four-body system that is related to the center-of-mass (c.m.) incident energy of ${}^8\text{B}$, E_{in} , with $E = E_{\text{in}} + e_7 + e_8$; e_8 is the eigenenergy of the ground state of ${}^8\text{B}$, i.e. -137 keV. The transition amplitude $\mathfrak{T}_{3\text{-body}}$ based on the three-body model is accurately obtained with CDCC [15, 16].

In actual CDCC calculation, the single-folding potential $U_{A7} = \langle \phi_7^{(0)} | U_{A3} + U_{A4} | \phi_7^{(0)} \rangle$ is replaced by the optical potential between A and ${}^7\text{Be}$. This replacement enables one to effectively include back-coupling of ${}^7\text{Be}$ breakup (or excitation) to the elastic channel, although it is very small for forward-scattering [15, 16]. Meanwhile, $V_{17} = \langle \phi_7^{(0)} | V_{13} + V_{14} | \phi_7^{(0)} \rangle$ is not uniquely determined yet, since V_{13} is rather ambiguous for the lack of data. However, this is not a problem in the present ANC analysis, because the C extracted from ${}^8\text{B}$ breakup is insensitive to the detail of V_{17} , as shown in Sec. III B.

As mentioned in Sec. I, the ground state of ${}^8\text{B}$ contains the $1/2^-$ excited-state of ${}^7\text{Be}$. In this configuration, the binding energy of p in ${}^8\text{B}$ is large, owing to the excitation energy of ${}^7\text{Be}$. The corresponding single-particle wave function thus falls-off rapidly as r increases, compared with that corresponding to the configuration where ${}^7\text{Be}$ is in the ground state. Hence, the ${}^8\text{B}$ wave function with the $1/2^-$ excited-state of ${}^7\text{Be}$ is irrelevant to the ANC approach to $S_{17}(0)$, where reactions are described only by wave functions in the tail region. Although this irrelevant component has finite contribution to ${}^8\text{B}$ breakup cross sections, fortunately, it is not included in the experimental data measured at RIKEN, GSI and MSU [7, 8, 9, 10, 11, 12, 13], as already mentioned. We have shown above that ${}^7\text{Be}$ can be assumed to be inert during the breakup process of ${}^8\text{B}$. Thus, by using Eq. (3), comparison between the result of CDCC based on the $p+{}^7\text{Be}+A$ three-body model and experimental data at forward angles can determine C , from which $S_{17}(0)$ is accurately determined by the ANC method with Eq. (2).

C. E-CDCC and hybrid scattering amplitude

In this subsection we describe the formalism of E-CDCC and how to construct a hybrid scattering-amplitude from the results of E-CDCC and fully quantum-mechanical CDCC. The following formulation contains two important extensions of E-CDCC. One is the inclusion of the intrinsic spin of the projectile and the other is more accurate treatment of the Coulomb wave function in coupled-channel equations than in the previous formulation of E-CDCC [33]. Detailed formal-

ism of CDCC and its theoretical foundation are shown elsewhere [15, 16, 38].

In consequence of the discussion in the previous subsection, we start with the three-body model shown in Fig. 2 for description of ${}^8\text{B}$ breakup. As already mentioned,

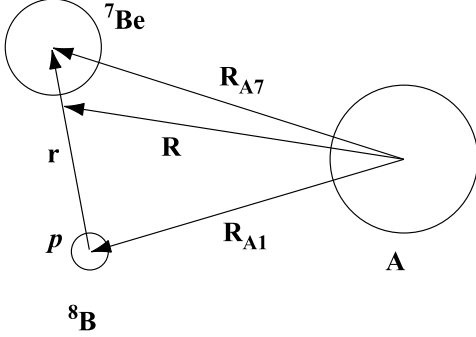


FIG. 2: Illustration of the $p+{}^7\text{Be}+A$ three-body system.

the total wave function $\Psi_{3\text{-body}}$ satisfies the three-body Schrödinger equation,

$$(H_{3\text{-body}} - E_{\text{in}} - e_8)\Psi_{3\text{-body}}(\mathbf{R}, \mathbf{r}) = 0. \quad (9)$$

We first expand $\Psi_{3\text{-body}}$ in terms of intrinsic wave-functions $\Phi_{i,\ell SI m}(\mathbf{r})$ of ${}^8\text{B}$:

$$\begin{aligned} \Psi_{3\text{-body}}(\mathbf{R}, \mathbf{r}) &= \sum_{i\ell SI m} \Phi_{i,\ell SI m}(\mathbf{r}) \\ &\times \sum_J e^{-i(m-m_0)\phi_R} \chi_{i\ell SI m}^J(R, \theta_R). \end{aligned} \quad (10)$$

Coefficients $\sum_J \chi_{i\ell SI m}^J(R, \theta_R) \exp[-i(m-m_0)\phi_R]$ of the expansion show the c.m. motion of the projectile in the $\{i, \ell, S, I, m\}$ channel, where ℓ, S and I are the orbital angular momentum, the channel-spin and the total spin of ${}^8\text{B}$, respectively; the orbital angular momentum between ${}^8\text{B}$ and A is denoted by L , and J is the total angular momentum of the three-body system. The symbol m is the projection of I on the z -axis taken to be parallel to the incident beam, and m_0 is m in the initial state. For simplicity we below denote the five channel-indices $\{i, \ell, S, I, m\}$ as c .

We take the same Φ_c as CDCC [15, 16] does, which consist of bound-states and “discretized-continuum-states.” As for the prescription for calculating the latter, the average method [15, 16, 17, 39] and the pseudo-state methods [15, 40, 41, 42] are most widely used. The Φ_c satisfy

$$\langle \Phi_{c'}(\mathbf{r}) | h | \Phi_c(\mathbf{r}) \rangle_{\mathbf{r}} = \epsilon_{i,\ell SI} \delta_{c'c}, \quad (11)$$

where h is the internal Hamiltonian defined by $h = T_r + V_{17}(\mathbf{r})$ and $\epsilon_{i,\ell SI}$ is the intrinsic energy corresponding to the channel $\{i, \ell, S, I\}$. As for the coupling scheme of angular momenta, we take the following form

$$\Phi_c(\mathbf{r}) = \varphi_{i,\ell SI}(r) [i^\ell Y_\ell(\hat{\mathbf{r}}) \otimes \zeta_S]_{Im}, \quad (12)$$

where $Y_{\ell m}$ is the spherical harmonics and ζ_S the spin wave function of the projectile with channel-spin S . It should be noted that $\Phi_0(\mathbf{r})$, where the subscript 0 represents the ground state of ${}^8\text{B}$, is nothing but $\psi_{17}(\mathbf{r})$ in Eq. (6), if $\Phi_0(\mathbf{r})$ has a single configuration; an expression of $\psi_{17}(\mathbf{r})$ with configuration-mixing is described in Sec. III B. Since the Φ_c are chosen to form an approximate complete-set in a finite space being significant for a reaction concerned [40], the expansion of Eq. (10) is assumed to be accurate. Unknown coefficients $\chi_c^J(R, \theta_R)$ of the expansion are obtained by solving coupled-channel equations derived below.

Multiplying Eq. (9) by $\Phi_{c'}^*(\mathbf{r})$ from the left and integrating over \mathbf{r} and internal coordinates concerned with the spin lead to coupled equations for χ_c^J :

$$\begin{aligned} \sum_J e^{-im'\phi_R} (\mathcal{T}_R + \epsilon_{c'} - E_{\text{in}} - e_8) \chi_c^J(R, \theta_R) \\ = - \sum_c F_{c'c} \sum_J e^{-im\phi_R} \chi_c^J(R, \theta_R). \end{aligned} \quad (13)$$

The reduced kinetic-energy operator \mathcal{T}_R and the form factor $F_{c'c}$, in the cylindrical coordinate taken here, are defined by

$$\mathcal{T}_R = -\frac{\hbar^2}{2\mu} \nabla_R^2 + \frac{\hbar^2}{2\mu} \frac{(m' - m_0)^2}{b^2} \approx -\frac{\hbar^2}{2\mu} \nabla_R^2 = T_R, \quad (14)$$

$$\begin{aligned} F_{c'c}(\mathbf{R}) &= \langle \Phi_{c'} | V_{A7} + V_{A1} | \Phi_c \rangle_{\mathbf{r}} \\ &\equiv \mathcal{F}_{c'c}(R, \theta_R) e^{-i(m' - m)\phi_R}. \end{aligned} \quad (15)$$

In Eq. (14) μ is the reduced mass of the ${}^8\text{B}$ - A system and the impact parameter b is given by $b = \sqrt{x^2 + y^2}$ for the vector $\mathbf{R} = (x, y, z)$; we have neglected the weak-dependence of \mathcal{T}_R on b , which turned out to have no effect on numerical results in the present case. In Eq. (15) we assume V_{A7} and V_{A1} to be central interactions; this assumption is valid, as discussed in Ref. [33], since we use E-CDCC only to obtain the scattering amplitude for large values of b . The explicit form of the coupling potentials $\mathcal{F}_{c'c}$ is then

$$\begin{aligned} \mathcal{F}_{c'c}(R, \theta_R) &= \sum_\lambda i^{\ell - \ell'} \sqrt{4\pi} (-)^{2I' + m - S} \\ &\times \sqrt{\frac{(2\ell + 1)(2\ell' + 1)(2I + 1)(2I' + 1)}{(2\lambda + 1)^3}} \\ &\times (I - m \ I' m' | \lambda \ m' - m) (\ell 0 \ell' 0 | \lambda 0) \\ &\times W(\ell \ell' I I'; \lambda S) \delta_{S' S} \\ &\times C_{\lambda m' - m} P_{\lambda m' - m}(\cos \theta_R) \\ &\times \int \varphi_{i', \ell' S' I'}^*(r) \mathcal{U}^{(\lambda)}(R, r) \varphi_{i, \ell S I}(r) r^2 dr, \end{aligned}$$

where $W(\ell \ell' I I'; \lambda S)$ is the Racah coefficient and

$$C_{\lambda \nu} \equiv (-)^{(\nu + |\nu|)/2} \sqrt{\frac{2\lambda + 1}{4\pi} \frac{(\lambda - |\nu|)!}{(\lambda + |\nu|)!}}.$$

The λ th-order multipole $\mathcal{U}^{(\lambda)}$ is defined by $\mathcal{U}^{(\lambda)}(R, r) = u_{A7}^{(\lambda)}(R, r/8) + u_{A1}^{(\lambda)}(R, 7r/8)$ with

$$U_{A7}(R_{A7}) = \sum_{\lambda} u_{A7}^{(\lambda)}(R, r/8) \frac{4\pi}{\lambda^2} \sum_{\nu} Y_{\lambda\nu}^*(\hat{\mathbf{R}}) Y_{\lambda\nu}(\hat{\mathbf{r}}),$$

$$U_{A1}(R_{A1}) = \sum_{\lambda} u_{A1}^{(\lambda)}(R, 7r/8) \frac{4\pi}{\lambda^2} \sum_{\nu} Y_{\lambda\nu}^*(\hat{\mathbf{R}}) Y_{\lambda\nu}(\hat{\mathbf{r}}).$$

Now we make the Coulomb-eikonal approximation [43] to χ_c^J :

$$\chi_c^J(R, \theta_R) \approx \xi_c^J(b, z) \phi_c^{C(+)}(b, z). \quad (16)$$

In Eq. (16) $\phi_c^{C(+)}$ is the outgoing Coulomb-wave-function:

$$\phi_c^{C(+)}(b, z) = \frac{e^{-\pi\eta_c/2}}{(2\pi)^{3/2}} \Gamma(1 + i\eta_c) e^{i\mathbf{K}_c \cdot \mathbf{R}} F_{\mathbf{K}_c}^c(\mathbf{R}),$$

$$F_{\mathbf{K}_c}^c(\mathbf{R}) \equiv G(-i\eta_c, 1, i(K_c R - \mathbf{K}_c \cdot \mathbf{R}))$$

with Γ the Gamma function and G the confluent hypergeometric function. In actual calculation we make use of the approximate asymptotic-form of $\phi_c^{C(+)}$,

$$\phi_c^{C(+)}(b, z) \sim \frac{1}{(2\pi)^{3/2}} \left(1 + \frac{\eta_c^2}{i(K_c R - \mathbf{K}_c \cdot \mathbf{R})} + \dots \right) \times e^{i(\mathbf{K}_c \cdot \mathbf{R} + \eta_c \ln(K_c R - \mathbf{K}_c \cdot \mathbf{R}))}$$

$$\approx \frac{1}{(2\pi)^{3/2}} e^{i(K_c z + \eta_c \ln(K_c R - K_c z))}, \quad (17)$$

which is valid for large values of b . The boundary condition for ξ_c^J in Eq. (16) is $\lim_{z \rightarrow -\infty} \xi_c^J(b, z) = \delta_{c0}$, where 0 denotes the incident channel. Then, the scattering wave-function χ_c^J satisfies the appropriate boundary condition at $z \rightarrow -\infty$.

We here make the following two approximations, just in the same way as in Ref. [33]. (i) For sufficiently large b , the flux of $\phi_c^{C(+)}$ is assumed to be parallel to the z -axis. (ii) We make the local semiclassical approximation [44] to $\phi_c^{C(+)}$,

$$\frac{\partial \phi_c^{C(+)}(b, z)}{\partial z} \approx iK_c(R) \phi_c^{C(+)}(R), \quad (18)$$

which is valid for a wave function under a slowly-varying potential. The local wave number $K_c(R)$ is defined by

$$\frac{\hbar^2}{2\mu} K_c^2(R) = E_{\text{in}} + e_8 - \epsilon_c - \frac{Z_8 Z_A e^2}{R}, \quad (19)$$

where $Z_8 e$ ($Z_A e$) represents the charge of ^8B (A). Further approximation to $\phi_c^{C(+)}$ was made in Ref. [33], i.e. the c -dependence of $F_{\mathbf{K}_c}^c$ was neglected. On the contrary, in the present paper we solve coupled-channel equations taking account of that dependence by using Eq. (17). This treatment of the Coulomb wave function turned out to slightly improve the agreement between the quantum-mechanical and eikonal scattering-amplitudes for large L .

In consequence of Eq. (14) and the Coulomb-eikonal approximation, one finds

$$\mathcal{T}_R \chi_c^J(R, \theta_R) \approx T_R \left(\xi_c^J(b, z) \phi_c^{C(+)}(b, z) \right)$$

$$\approx \left[-\frac{i\hbar^2}{\mu} K_c(R) \left(\frac{\partial \xi_c^J(b, z)}{\partial z} \right) + \left(T_R \phi_c^{C(+)}(b, z) \right) \xi_c^J(b, z) \right] \phi_c^{C(+)}(b, z), \quad (20)$$

where the second-order derivative of ξ_c^J has been neglected since it is slowly varying compared with the remainder $\phi_c^{C(+)}(b, z)$. Inserting Eqs. (15), (17), (20) and

$$T_R \phi_c^{C(+)}(b, z) = \left(E_{\text{in}} + e_8 - \epsilon_c - \frac{Z_8 Z_A e^2}{R} \right) \phi_c^{C(+)}(b, z) \quad (21)$$

into Eq. (13), one reaches to the following coupled-channel equations

$$\frac{i\hbar^2}{\mu} K_c(R) \frac{d}{dz} \psi_c^{(b)}(z) = \sum_{c'} \mathfrak{F}_{cc'}^{(b)}(z) \mathcal{R}_{cc'}^{(b)}(z) \psi_{c'}^{(b)}(z) \times e^{i(K_{c'} - K_c)z}, \quad (22)$$

where $\psi_c^{(b)}(z) \equiv \sum_J \xi_c^J(b, z)$; we have put the non-dynamical variable b in a superscript and commuted c and c' . The reduced coupling-potential $\mathfrak{F}_{cc'}$ is defined by

$$\mathfrak{F}_{cc'}^{(b)}(z) = \mathcal{F}_{cc'}^{(b)}(z) - \frac{Z_8 Z_A e^2}{R} \delta_{cc'} \quad (23)$$

and

$$\mathcal{R}_{cc'}^{(b)}(z) \equiv \frac{e^{i\eta_{c'} \ln(K_{c'} R - K_{c'} z)}}{e^{i\eta_c \ln(K_c R - K_c z)}} = \frac{(K_{c'} R - K_{c'} z)^{i\eta_{c'}}}{(K_c R - K_c z)^{i\eta_c}}. \quad (24)$$

Since the E-CDCC equation has the first-order differential form and contains no coefficient with huge angular-momentum, one can solve it with high computational speed and accuracy.

The eikonal scattering amplitude with Coulomb distortion is given by $f_{c0}^E = f_{c0}^{\text{Ruth}} \delta_{c0} + f_{c0}^E$, where f_{c0}^{Ruth} is the Rutherford amplitude and

$$f_{c0}^E \equiv -\frac{(2\pi)^2 \mu}{\hbar^2} \int \sum_{c'} \mathfrak{F}_{cc'}^{(b)}(z) \phi_c^{*C(-)}(b, z) \phi_{c'}^{C(+)}(b, z) \times e^{-i(m-m_0)\phi_R} \psi_{c'}^{(b)}(z) d\mathbf{R} \quad (25)$$

with

$$\phi_c^{C(-)}(b, z) = \frac{e^{-\pi\eta_c/2}}{(2\pi)^{3/2}} \Gamma^*(1 + i\eta_c) e^{i\mathbf{K}_c' \cdot \mathbf{R}} F_{-\mathbf{K}_c'}^{*c}(\mathbf{R})$$

$$\approx \frac{1}{(2\pi)^{3/2}} e^{i\mathbf{K}_c' \cdot \mathbf{R}} e^{-i\eta_c \ln(K_c R + \mathbf{K}_c' \cdot \mathbf{R})}. \quad (26)$$

The outgoing c.m. momentum $\hbar\mathbf{K}'_c$ is chosen to be on the z - x plane, following the Madison convention. We here assume forward scattering just in the same way as in Ref. [33], i.e. the phase-factor $(\mathbf{K}_{c'} - \mathbf{K}'_c) \cdot \mathbf{R}$, which appears in $\phi_c^{*C(-)}(b, z)\phi_{c'}^{C(+)}(b, z)$, is approximated by $-K_c\theta_f b \cos\phi_R + (K_{c'} - K_c)z$, where θ_f is the scattering angle of ${}^8\text{B}$. Furthermore, we replace $K_c R + \mathbf{K}'_c \cdot \mathbf{R}$ in Eq. (26) by $K_c R + K_c z$. One then finds

$$f'_{c0}{}^E = -\frac{\mu}{2\pi\hbar^2} \int e^{-i(m-m_0)\phi_R} e^{-iK_c \sin\theta_f b \cos\phi_R} b db d\phi_R \\ \times \mathcal{H}_c^{(b)} \int \sum_{c'} \mathfrak{F}_{cc'}^{(b)}(z) \psi_{c'}^{(b)}(z) e^{i(K_{c'} - K_c)z} \mathcal{R}_{cc'}^{(b)}(z) dz, \quad (27)$$

with $\mathcal{H}_c^{(b)} \equiv \exp[2i\eta_c \ln(K_c b)]$.

The integration over z in Eq. (27) can be done analytically with the help of Eq. (22), i.e.

$$\mathcal{I} \equiv \int \sum_{c'} \mathfrak{F}_{cc'}^{(b)}(z) \psi_{c'}^{(b)}(z) e^{i(K_{c'} - K_c)z} \mathcal{R}_{cc'}^{(b)}(z) dz \\ = \frac{i\hbar^2}{\mu} \int K_c(R) \left(\frac{d}{dz} \psi_c^{(b)}(z) \right) dz \\ \approx \frac{i\hbar^2}{\mu} \left[K_c(R) \psi_c^{(b)}(z) \right]_{-\infty}^{\infty} \\ \equiv \frac{i\hbar^2}{\mu} K_c \left[\mathcal{S}_{c0}^{(b)} - \delta_{c0} \right], \quad (28)$$

where we have neglected $\partial K_c(R)/\partial z$, since $K_c(R)$, with large b , is a slowly-varying function of z . The eikonal S -matrix elements are defined by $\mathcal{S}_{c0}^{(b)} = \lim_{z \rightarrow \infty} \psi_c^{(b)}(z)$. Inserting Eq. (28) into Eq. (27) leads to

$$f'_{c0}{}^E \approx \frac{K_c}{2\pi i} \int e^{-i(m-m_0)\phi_R} e^{-iK_c \sin\theta_f b \cos\phi_R} b db d\phi_R \\ \times \mathcal{H}_c^{(b)} \left[\mathcal{S}_{c0}^{(b)} - \delta_{c0} \right]. \quad (29)$$

We here transform the integration over b to the summation over L , just in the same way as in Ref. [33]. The resulting eikonal amplitude is

$$f'_{c0}{}^E = \frac{2\pi}{iK_0} \sum_L \frac{K_0}{K_c} \mathcal{H}_c^{(b_{c;L})} \sqrt{\frac{2L+1}{4\pi}} i^{(m-m_0)} \\ \times \left[\mathcal{S}_{c0}^{(b_{c;L})} - \delta_{c0} \right] Y_{L m-m_0}(\hat{\mathbf{K}}') \\ \equiv \frac{2\pi}{iK_0} \sum_L f'_{L;c0}{}^E Y_{L m-m_0}(\hat{\mathbf{K}}') \quad (30)$$

with $K_c b_{c;L} = L + 1/2$. The quantum-mechanical scattering amplitude, which is obtained by CDCC, is given

by

$$f'_{c0}{}^Q = \frac{2\pi}{iK_0} \sum_L \sum_{J=|L-I|}^{L+I} \sum_{L_0=|J-I_0|}^{J+I_0} \sqrt{\frac{2L_0+1}{4\pi}} \\ \times (I_0 m_0 L_0 0 | J m_0) (I m L m_0 - m | J m_0) \\ \times (S_{iLlSI, i_0 L_0 \ell_0 S_0 I_0}^J - \delta_{i_0} \delta_{LL_0} \delta_{\ell_0} \delta_{SS_0} \delta_{II_0}) \\ \times e^{i(\sigma_L + \sigma_{L_0})} (-)^{m-m_0} Y_{L m-m_0}(\hat{\mathbf{K}}') \\ \equiv \frac{2\pi}{iK_0} \sum_L f'_{L;c0}{}^Q Y_{L m-m_0}(\hat{\mathbf{K}}'), \quad (31)$$

where σ_L is the Coulomb phase shift. The hybrid scattering amplitude is defined by

$$f'_{c0}{}^H = f'_{c0}{}^{\text{Ruth}} \delta_{c0} + \frac{2\pi}{iK_0} \sum_{L < L_C} f'_{L;c0}{}^Q Y_{L m-m_0}(\hat{\mathbf{K}}') \\ + \frac{2\pi}{iK_0} \sum_{L \geq L_C} f'_{L;c0}{}^E Y_{L m-m_0}(\hat{\mathbf{K}}'), \quad (32)$$

which is used in the present analysis of ${}^8\text{B}$ breakup. The connecting-angular-momentum L_C between quantum-mechanical and eikonal amplitudes is chosen so that $f'_{L;c0}{}^E$ agrees with $f'_{L;c0}{}^Q$ for $L \geq L_C$. It should be noted that Eq. (32) includes all quantum effects and also the interference between amplitudes in the two L -regions. This hybrid CDCC calculation turned out to describe nuclear and Coulomb breakup with very high accuracy and computational speed. Actually, it was found that the accuracy is the same as that of fully quantum-mechanical CDCC and the computation time is almost as 1/10 as that of standard CDCC calculation.

III. RESULTS AND DISCUSSION

A. Analysis of ${}^8\text{B}$ breakup experiment

Inputs for the calculation of ${}^{208}\text{Pb}({}^8\text{B}, p+{}^7\text{Be}){}^{208}\text{Pb}$ at 52 MeV/nucleon with CDCC and E-CDCC are as follows. We adopt a single-particle model for the ${}^8\text{B}$ wave function. The intrinsic spins of ${}^7\text{Be}$ and p are neglected, which means that we do not distinguish between the ${}^7\text{Be}(3/2^-) \otimes p(1/2^-)$ and the ${}^7\text{Be}(3/2^-) \otimes p(3/2^-)$ configurations in the ground state of ${}^8\text{B}$. Thus, the asymptotic normalization coefficient obtained below directly corresponds to C in Eq. (2). Effects of the intrinsic spins on $S_{17}(0)$ are discussed in Sec. III B. The single-particle potential of Esbensen and Bertsch (EB) [45] is used for the p-state of ${}^8\text{B}$. We adjust the depth of the potential to reproduce the separation energy of p , 137 keV. For the s- and d-states we use the potential of Barker [46]; the resulting scattering length \bar{a}_s is -8 fm, which is consistent with the experimental value, i.e. -7 ± 3 fm [47]. We assume the potential for the f-state is the same as that for the d-state. We found by numerical calculation that the results shown below are essentially independent of the single-particle potentials for the d- and

f-states. As for the distorting potential between p (${}^7\text{Be}$) and ${}^{208}\text{Pb}$ we adopt the global optical potential by Koning and Delaroche [48] (Cook [49]). We neglect the spin-orbit parts of the p - ${}^{208}\text{Pb}$ potential; this approximation is expected to have no effect on the resulting $S_{17}(0)$, since the ANC analysis uses the experimental data below 2° where nuclear coupling-potentials can essentially be neglected, as one sees below. The multipoles for nuclear and Coulomb coupling-potentials are included up to $\lambda = 6$. The discretized-continuum states of ${}^8\text{B}$ are constructed by the average method [15, 16, 17, 39]. The maximum excitation energy of ${}^8\text{B}$ is 10 MeV; 10, 20, 10 and 5 discretized-continuum states are taken for $\ell = 1, 0, 2$ and 3 states, respectively, and the resulting number of scattering-channels in CDCC is 138. The maximum values of r , R and L are, respectively, 200 fm, 1000 fm and 12000. The above modelspace turned out to give good convergence of the resulting breakup-cross-section.

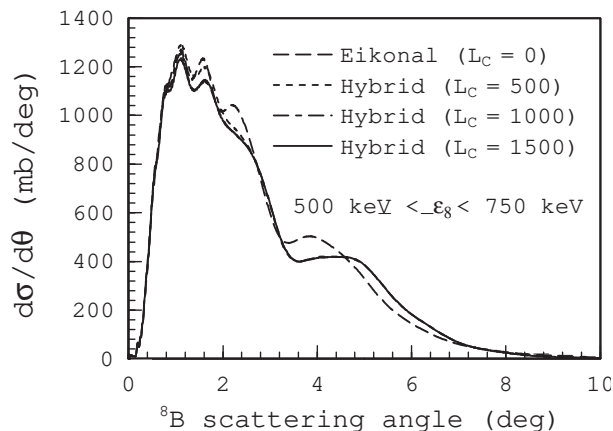


FIG. 3: The ${}^8\text{B}$ breakup cross section as a function of the scattering angle of the c.m. of ${}^8\text{B}$. The cross section has been integrated over the excitation energy of ${}^8\text{B}$, ε_8 , measured from the $p+{}^7\text{Be}$ threshold energy, in the range of 500–750 keV. The dotted, dash-dotted and solid lines represent the results of the hybrid calculation of CDCC and E-CDCC with $L_C = 500, 1000$ and 1500 , respectively. The result of E-CDCC, i.e. $L_C = 0$, is also shown by the dashed line.

Figure 3 shows the convergence of the hybrid calculation with CDCC and E-CDCC. The dashed line is the result of E-CDCC calculation ($L_C = 0$) of the ${}^8\text{B}$ breakup cross section, as a function of the scattering angle of ${}^8\text{B}$, θ_8 . The cross section has been integrated over the excitation energy of ${}^8\text{B}$, ε_8 , from 500 keV to 750 keV. The dotted, dash-dotted and solid lines correspond to the hybrid calculation with $L_C = 500, 1000$ and 1500 , respectively. The figure shows that the hybrid calculation converges with $L_C = 1000$. The difference between the dash-dotted and solid lines is only less than about 1% in magnitude. Thus, below we regard the hybrid calculation of CDCC and E-CDCC with $L_C = 1000$ as the fully quantum-mechanical CDCC calculation.

One sees in Fig. 3 the oscillation of the cross section at

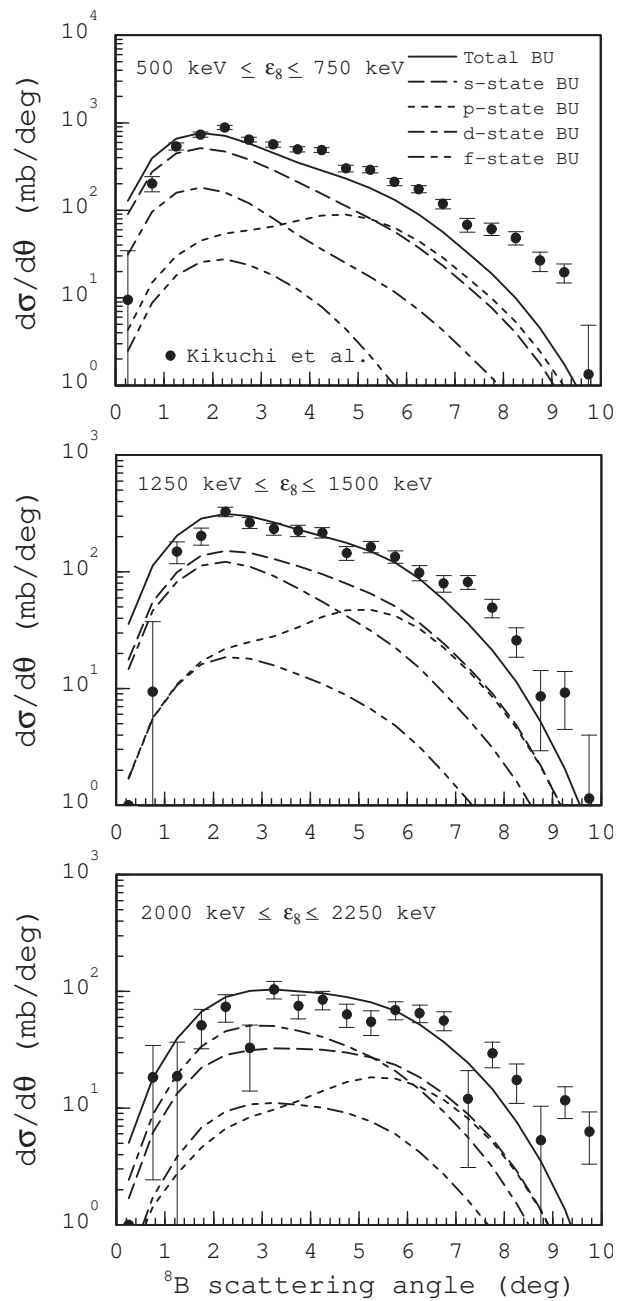


FIG. 4: Angular distribution of the energy-integrated ${}^8\text{B}$ breakup cross section. The top, middle and bottom panels correspond to the integration-range over ε_8 of 500–750 keV, 1250–1500 keV and 2000–2250 keV, respectively. In each panel the dashed, dotted, dash-dotted and dash-two-dotted lines represent the breakup cross sections to the s-, p-, d- and f-states of ${}^8\text{B}$, respectively, and the solid line is the sum of them. The calculated cross sections are smeared out by taking account of the resolution and efficiency of the measurement [50]. The experimental data are taken from Ref. [8].

forward angles around 2° , which turned out to be due to the interference between nuclear and Coulomb breakup-amplitudes. Therefore, one can conclude that nuclear interactions affect the breakup cross section even at very forward angles. However, as one sees below, this oscillation is not observed in actual experimental data owing to the limit of the resolution of θ_8 for the measurement.

Figure 4 shows the comparison between CDCC calculation and the experimental data for the ^8B breakup. In order to take account of the experimental resolution and efficiency, the theoretical result has been smeared out by using the filtering-table [50] provided by the authors of Ref. [8]. The top, middle and bottom panels correspond to the integration-range over ε_8 of 500–750 keV, 1250–1500 keV and 2000–2250 keV, respectively. The dashed, dotted, dash-dotted and dash-two-dotted lines in each panel are, respectively, the breakup cross sections of ^8B to its s-, p-, d- and f-states, and the solid line is the sum of them. One sees the CDCC calculation well reproduces the experimental data except at backward angles in the top panel, where the calculation quite underestimates the data. Reason for this underestimation is discussed in Sec. III C.

One also sees from Fig. 4 that the s- and d-state breakup cross sections are dominant up to about 4° , which shows the importance of the E1 breakup processes of ^8B . However, in the top panel, i.e. for $500 \text{ keV} \leq \varepsilon_8 \leq 750 \text{ keV}$, the d-state breakup cross section is much smaller than the s-state one. This is because the centrifugal barrier for the d-state ($\sim 9 \text{ MeV}$) hinders the breakup process for such low excitation-energies. It should be noted that the filtering-table used was made

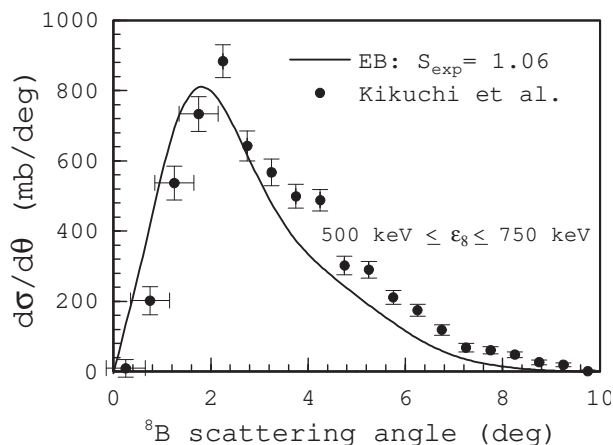


FIG. 5: The result of the χ^2 -fit of the breakup cross section for $500 \text{ keV} \leq \varepsilon_8 \leq 750 \text{ keV}$ calculated with the ^8B single-particle potential of Esbensen and Bertsch (EB) [45]. The solid line is the same as that in the top panel in Fig. 4 but multiplied by the spectroscopic factor $\mathfrak{S}_{\text{exp}} = 1.06$. For the four data points below 2° , which are used in the fitting procedure, we put the horizontal error-bar corresponding to the resolution of θ_8 [8] for the measurement.

with assuming the s-state breakup of ^8B . Thus, quantitative comparison between the calculation and the experimental data, to extract $S_{17}(0)$ with less than 5% in error, can only be done in the region where the s-state breakup cross section is dominant. For this reason below we use the low-energy breakup data for $\theta_8 \leq 2^\circ$ to determine $\mathfrak{S}_{\text{exp}}$ by Eq. (3). We here note that resonance states of ^8B , which are not well understood at this stage, affect the breakup cross section for $\theta_8 > 2^\circ$, as one sees in Sec. III C.

Figure 5 shows the result of the χ^2 -fit of the theoretical calculation to the experimental data. The solid line is the same as that in the top panel in Fig. 4 but multiplied by the spectroscopic factor $\mathfrak{S}_{\text{exp}} = 1.06$. It should be noted that in the χ^2 -fitting procedure we have taken account of 0.4° experimental error of θ_8 [8], shown by the horizontal error-bars in Fig. 5, and minimized the value of χ^2 . The single-particle ANC corresponding to the EB ^8B wave-function is $\alpha = 0.712 \text{ fm}^{-1/2}$. With these values of $\mathfrak{S}_{\text{exp}}$ and α , the value of the ANC C is obtained from Eq. (3), i.e. $C = 0.732 \text{ fm}^{-1/2}$. One can then determine $S_{17}(0)$ by inserting this result into Eq. (2), together with the value of the scattering length $\bar{a}_s = -8.0 \text{ fm}$, i.e. $S_{17}(0) = 20.6 \text{ eV b}$. In the next subsection we quantitatively evaluate uncertainties of the extracted $S_{17}(0)$ and make a correction on it due to roles of the intrinsic spin of ^8B .

B. Uncertainties of the extracted $S_{17}(0)$ and effects of the intrinsic spin of ^8B

First, we evaluate the uncertainty of $S_{17}(0)$ that comes from the use of the ANC method, just in the same way as in Refs. [25, 28]. We show in Fig. 6 the result of CDCC

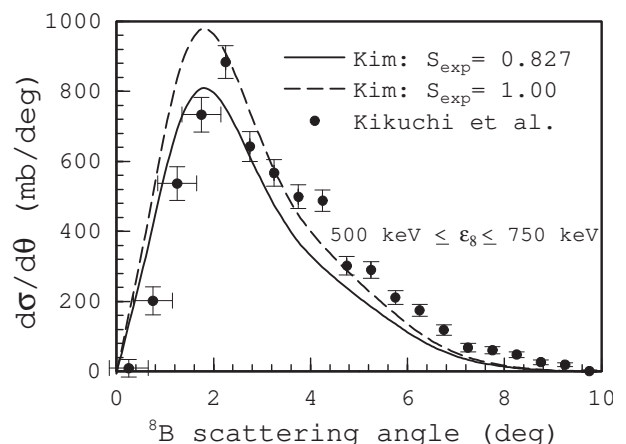


FIG. 6: Same as in Fig. 5 but for the CDCC calculation with Kim's single-particle potential [51] for the p-state of ^8B ; the spectroscopic factor obtained is 0.827. The result with Kim's potential before χ^2 -fitting, namely with $\mathfrak{S}_{\text{exp}} = 1.00$, is also shown by the dashed line for comparison.

calculation with the p-state single-particle potential of ^8B by Kim *et al.* [51] (the dashed line) and that multiplied by $\mathfrak{S}_{\text{exp}} = 0.827$ (the solid line); the latter agrees with the result shown in Fig. 5 within 1% in error. One sees that $\mathfrak{S}_{\text{exp}}$ indeed depends on the p-state potential. Actually, the single-particle ANC for Kim's potential is $0.805 \text{ fm}^{-1/2}$, which quite differs from the value for the EB potential, $0.712 \text{ fm}^{-1/2}$, because of the difference in geometry of the two potentials of about 20%. On the contrary, the resulting value of ANC with Kim's potential is $0.732 \text{ fm}^{-1/2}$ that perfectly agrees with the result shown in Sec. III A. This result shows that the ANC method works with very high accuracy in the present analysis, i.e. the error of the ANC method is negligibly small.

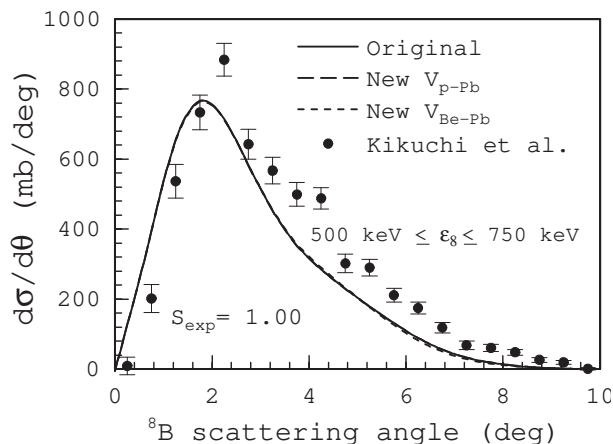


FIG. 7: Dependence of the ^8B breakup cross section on the distorting potentials used in CDCC. The solid line is the same as that in the top panel in Fig. 4. The dashed (dotted) line represents the result with an alternative distorting potential for $p\text{-}^{208}\text{Pb}$ ($^7\text{Be}\text{-}^{208}\text{Pb}$). The spectroscopic factor is taken to be unity for all calculations.

Second, we estimate effects of ambiguity of the distorting potentials used in the CDCC calculation on $S_{17}(0)$. For this purpose we prepare alternative optical potentials for $p\text{-}^{208}\text{Pb}$ and $^7\text{Be}\text{-}^{208}\text{Pb}$ elastic scattering. For the former, we modify the parameter set of Koning and Delaroche so that the calculated elastic cross section without spin-orbit terms reproduces the result with the full components of the optical potential. The parameter set thus obtained is $V_V = 39.82 \text{ MeV}$, $W_V = 0.776 \text{ MeV}$ and $W_D = 13.47 \text{ MeV}$, with the same notation as in Ref. [48]; all other parameters are not changed. For the latter, we use a single-folding model with the nucleon- ^{208}Pb potential of Koning and Delaroche. The density distribution of ^7Be is assumed to be the Gaussian form and the range of the Gaussian is determined to reproduce the rms matter radius of ^7Be , 2.48 fm [52].

Figure 7 shows the results of CDCC calculation with the new $p\text{-}^{208}\text{Pb}$ (the dashed line) and $^7\text{Be}\text{-}^{208}\text{Pb}$ (the dotted line) potentials. The result with the original inputs described in Sec. III A is also shown by the solid

line. The difference among the three lines is hardly visible. Therefore, we conclude that the error of $S_{17}(0)$ that comes from the ambiguity of the distorting potentials is negligibly small in the present case.

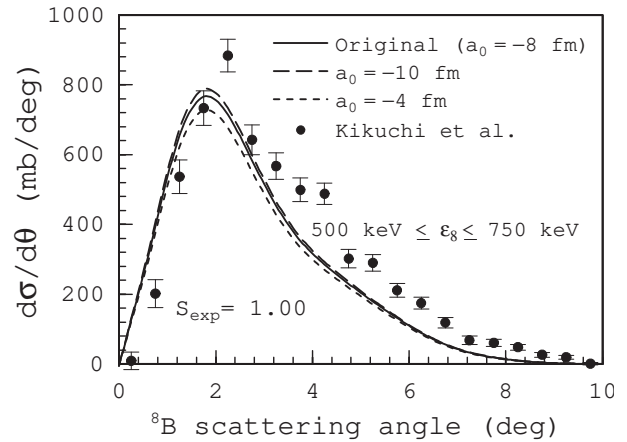


FIG. 8: Dependence of the ^8B breakup cross section on the single-particle potential for the s-state of ^8B . The solid line represents the result with Barker's potential that corresponds to the scattering length \bar{a}_s of -8 fm . The dashed (dotted) line shows the result with the s-state potential corresponding to $\bar{a}_s = -10$ (-4) fm .

Third, we discuss the ambiguity of the s-state single-particle potential of ^8B . We estimate the uncertainty of $S_{17}(0)$ concerned with this ambiguity by changing the depth of the s-state potential ranging from 52.80 MeV to 57.55 MeV , which corresponds to the range of the resulting scattering-length \bar{a}_s from -10 fm to -4 fm , i.e. the range of the experimental value of \bar{a}_s [47]. In Fig. 8 the solid, dashed and dotted lines represent the results with the s-state potentials correspond to $\bar{a}_s = -8$, -10 and -4 fm , respectively. One sees the breakup cross section slightly depends on the choice of the s-state potential of ^8B ; the resulting $S_{17}(0)$ is found to vary from 20.0 eV b to 21.5 eV b . Thus, we evaluate the error of $S_{17}(0)$ to be $+4.5\%/-2.6\%$.

Finally, we investigate effects of the intrinsic spins of p and ^7Be on $S_{17}(0)$. As mentioned in Sec. III A, $\psi_{17}(\mathbf{r}) \equiv \langle \phi_7^{(0)}(\mathbf{r}_{43}) | \phi_8^{(0)}(\mathbf{r}_{43}, \mathbf{r}) \rangle$ contains the following two configurations: (a) $^7\text{Be}(3/2^-) \otimes p(1/2^-)$ and (b) $^7\text{Be}(3/2^-) \otimes p(3/2^-)$. It should be noted that the possible $^7\text{Be}(1/2^-) \otimes p(3/2^-)$ configuration in the ground state of ^8B is not included in both theoretical calculation and experimental data in the present analysis. In asymptotic

region $r > R_N$, $\psi_{17}(\mathbf{r})$ is written by

$$\begin{aligned} \psi_{17}(\mathbf{r}) = & \left\{ C_{\frac{1}{2}} \left[\left[iY_1(\hat{\mathbf{r}}) \otimes \varsigma_{\frac{1}{2}} \right]_{\frac{1}{2}} \otimes \varsigma_{\frac{3}{2}} \right]_{2m_0} \right. \\ & \left. + C_{\frac{3}{2}} \left[\left[iY_1(\hat{\mathbf{r}}) \otimes \varsigma_{\frac{1}{2}} \right]_{\frac{3}{2}} \otimes \varsigma_{\frac{3}{2}} \right]_{2m_0} \right\} \\ & \times \frac{W_{-\eta, 3/2}(2k_0 r)}{r}, \end{aligned} \quad (33)$$

where $\varsigma_{1/2}$ ($\varsigma_{3/2}$) is the spin- $\frac{1}{2}$ (spin- $\frac{3}{2}$) wave function. The ratio of the ANC for configuration (a) to that for (b) is determined by microscopic calculation [29], i.e. $C_{1/2}^2/C_{3/2}^2 = 0.157$. In actual calculation, as already mentioned, we take a normalized single particle wave function for the radial part of $\psi_{17}(\mathbf{r})$, which in principle depends on the configuration of ${}^8\text{B}$. However, as shown above, $S_{17}(0)$ is determined from the theoretical and experimental results at forward angles, where the inner part of the ${}^8\text{B}$ wave function has no contribution. Therefore, instead of Eq. (33), one can use

$$\begin{aligned} \psi_{17}(\mathbf{r}) = & \left\{ P \left[\left[iY_1(\hat{\mathbf{r}}) \otimes \varsigma_{\frac{1}{2}} \right]_{\frac{1}{2}} \otimes \varsigma_{\frac{3}{2}} \right]_{2m_0} \right. \\ & \left. + Q \left[\left[iY_1(\hat{\mathbf{r}}) \otimes \varsigma_{\frac{1}{2}} \right]_{\frac{3}{2}} \otimes \varsigma_{\frac{3}{2}} \right]_{2m_0} \right\} \frac{f_0(r)}{r} \end{aligned}$$

with $f_0(r)$ is a normalized radial wave-function and $P^2 = C_{1/2}^2/(C_{1/2}^2 + C_{3/2}^2) \sim 0.136$ and $Q^2 = C_{3/2}^2/(C_{1/2}^2 + C_{3/2}^2) \sim 0.864$. Transformation of the coupling scheme of angular-momenta leads to

$$\begin{aligned} \psi_{17}(\mathbf{r}) = & \left\{ P' \left[iY_1(\hat{\mathbf{r}}) \otimes \left[\varsigma_{\frac{1}{2}} \otimes \varsigma_{\frac{3}{2}} \right]_{S=1} \right]_{2m_0} \right. \\ & \left. + Q' \left[iY_1(\hat{\mathbf{r}}) \otimes \left[\varsigma_{\frac{1}{2}} \otimes \varsigma_{\frac{3}{2}} \right]_{S=2} \right]_{2m_0} \right\} \frac{f_0(r)}{r}, \end{aligned} \quad (34)$$

where

$$\begin{aligned} P' &= -\sqrt{6}W(1\ 2\ 1/2\ 1/2; 1\ 3/2)P \\ &\quad + 2\sqrt{3}W(1\ 2\ 1/2\ 3/2; 1\ 3/2)Q \\ &\sim 0.397, \\ Q' &= \sqrt{10}W(2\ 2\ 1/2\ 1/2; 1\ 3/2)P \\ &\quad - 2\sqrt{5}W(2\ 2\ 1/2\ 3/2; 1\ 3/2)Q \\ &\sim 0.918. \end{aligned}$$

As mentioned in Sec. III A, in the present analysis one can neglect spin-dependent interactions between the target nucleus and each constituent of ${}^8\text{B}$, which means that the channel-spin S is fixed during the breakup process of ${}^8\text{B}$ [15]. Thus, one can separately treat the $S = 1$ and $S = 2$ configurations in Eq. (34) and calculate breakup

cross sections corresponding to them: $\sigma_{S=1}$ and $\sigma_{S=2}$. Furthermore, if the p - ${}^7\text{Be}$ interaction is independent of S and I , obviously both $\sigma_{S=1}$ and $\sigma_{S=2}$ agree with the cross section σ_0 calculated with neglecting the intrinsic spin of ${}^8\text{B}$. For low excitation-energy breakup process, i.e. $500\text{ keV} \leq \varepsilon_8 \leq 750\text{ keV}$, p - ${}^7\text{Be}$ interactions V_{17} for the d- and f-states turned out to have no effect on the resulting breakup-cross-section. Moreover, V_{17} for the s-state of ${}^8\text{B}$ used in the spin-independent CDCC calculation above is chosen to reproduce the p - ${}^7\text{Be}$ scattering length for the $S = 2$ channel, i.e. $a_s^{S=2} = -7 \pm 3\text{ fm}$; we here note that in Ref. [47] the value of $a_s^{S=2}$ was regarded as the averaged scattering-length \bar{a}_s . Therefore, one sees $\sigma_{S=2} = \sigma_0$ in the present case. On the contrary, $\sigma_{S=1}$ is expected to differ from σ_0 because of the S -dependence of V_{17} for the s-state of ${}^8\text{B}$. Actually, the experimental result of $a_s^{S=1} = 25 \pm 9\text{ fm}$ [47] is quite different from that of $a_s^{S=2}$.

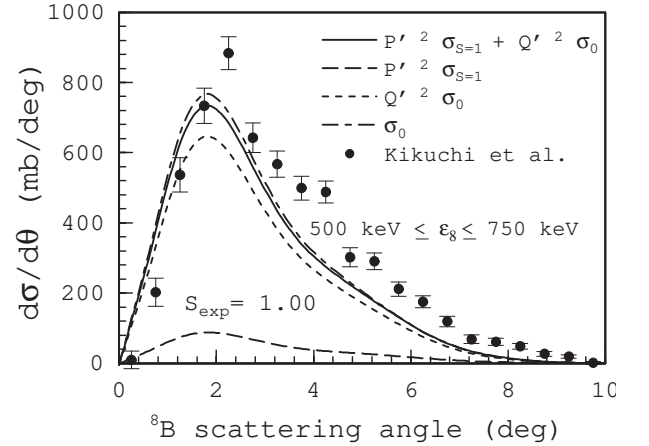


FIG. 9: The breakup cross section with the channel-spin $S = 1$, weighted by $P'^2 = 0.158$, is shown by the dashed line. The cross section corresponding to $S = 2$, which is equal to the S -independent cross section σ_0 , is shown by the dash-dotted line. The dotted line represents σ_0 multiplied by the mixing-factor $Q'^2 = 0.843$ and the solid line is the sum of the dashed and dotted lines.

Since the role of the intrinsic spin of ${}^8\text{B}$ can be evaluated from the difference between $\sigma_{S=1}$ and σ_0 , we calculated $\sigma_{S=1}$ by CDCC as follows. We include only the s- and p-states of ${}^8\text{B}$ and put the depth of V_{17} for the s-state to be 25.7 MeV so that the resulting scattering-length is consistent with the experimental result: $a_s^{S=1} = 25\text{ fm}$. The resulting number of the scattering-channels is 155. All other inputs are the same as in Sec. III A. The change in V_{17} for the s-state turned out to have no effect on the d- and f-state breakup cross sections. Hence, $\sigma_{S=1}$ can be calculated by taking the incoherent sum of $\sigma_{S=1}$ for the s- and p-states and σ_0 for the d- and f-states. On the other hand, as mentioned above, $\sigma_{S=2}$ is exactly equal to σ_0 . Thus, with Eq. (34) one can calculate the cross

section σ that takes account of the intrinsic spin of ${}^8\text{B}$:

$$\sigma = P'^2 \sigma_{S=1} + Q'^2 \sigma_0.$$

The results of $P'^2 \sigma_{S=1}$, $Q'^2 \sigma_0$ and σ are shown in Fig. 9 by the dashed, dotted and solid lines, respectively; σ_0 is also shown by the dash-dotted line. One sees, by comparing the solid line with the dash-dotted one, that the inclusion of the intrinsic spin of ${}^8\text{B}$ slightly decreases the breakup cross section. The χ^2 -fit of the solid line to the experimental data, just in the same way as in Sec. III A, results in $\mathfrak{S}_{\text{exp}} = 1.11$, which is somewhat larger than the result of the spin-independent calculation: $\mathfrak{S}_{\text{exp}} = 1.06$. Additionally, following Ref. [34], the value of \bar{a}_s in Eq. (2) corresponding to the spin-dependent ANC analysis is

$$\bar{a}_s = P'^2 a_s^{S=1} + Q'^2 a_s^{S=2} \sim -2.8 \text{ fm},$$

which is quite different from that used in the spin-independent analysis, i.e. -8 fm. One sees from Eq. (2) that this difference in \bar{a}_s makes $S_{17}(0)$ decrease by about 0.67%. Thus, one finds the following correction-factor

$$\mathfrak{C} \equiv \frac{1.11}{1.06} \times \frac{1 - 0.0013 \times (-2.8)}{1 - 0.0013 \times (-8)} \sim 1.04,$$

i.e. the result of $S_{17}(0) = 20.6$ eV b derived by the spin-independent calculation must be multiplied by \mathfrak{C} . The uncertainty of \mathfrak{C} corresponding to the experimental error of $a_s^{S=1}$ is evaluated from the fluctuation of \mathfrak{C} by changing V_{17} for the s-state of ${}^8\text{B}$ with $S = 1$ from 23.3 MeV to 30.5 MeV, which covers the range of the experimental value of $a_s^{S=1}$, i.e. 25 ± 9 fm. The result of \mathfrak{C} thus obtained is: $\mathfrak{C} = 1.04 \pm 0.01$.

The main result of $S_{17}(0)$ in the present paper is derived as follows. The central value of $S_{17}(0)$, including the correction factor \mathfrak{C} , is 21.4 eV b, which is consistent with the result of the recent precise measurement of ${}^7\text{Be}(p, \gamma){}^8\text{B}$ [4], $S_{17}(0) = 22.1 \pm 0.6$ (expt) ± 0.6 (theo) eV b. The theoretical error of the extracted $S_{17}(0)$ consists of two parts: one is concerned with the p - ${}^7\text{Be}$ scattering length for the $S = 2$ channel (+4.5%/-2.6%) and the other is due to the uncertainty of \mathfrak{C} (+0.6%/-0.8%), which in origin comes from the ambiguity of the scattering length for the $S = 1$ channel. Additionally, the extracted $S_{17}(0)$ has 8.4% systematic experimental error. Thus, we obtain

$$S_{17}(0) = 21.4_{-0.57}^{+0.96} \text{ (theo)} \pm 1.80 \text{ (expt)} \text{ eVb},$$

which is the main conclusion of the present paper.

C. Effects of resonance states of ${}^8\text{B}$

As mentioned in Sec. III A, the CDCC calculation underestimates the experimental data at backward angles. In Ref. [8] the behavior of the breakup cross section at backward angles was discussed from the viewpoint of the

nuclear breakup and Coulomb quadrupole (E2) excitation. Since the present CDCC calculation has already included the two components, one must seek another reason for the underestimation. The fact that the p-state breakup cross section exceeds the s-state one at backward angles suggests the importance of accurate description of the p-state wave function of ${}^8\text{B}$, which has the 1^+ and 3^+ resonances at 0.7695 MeV and 2.32 MeV, respectively. In order to see effects of these resonance states on the breakup cross section, we have extended the model-space of the CDCC calculation as follows. We include the intrinsic spins of p ($s_1 = 1/2$) and ${}^7\text{Be}$ ($s_7 = 3/2$) and assume the channel-spin S of ${}^8\text{B}$ to be 2. We then couple $S = 2$ with $\ell = 1$ and construct the 1^+ , 2^+ and 3^+ states. For 1^+ and 3^+ states we use the single-particle potential by Typel *et al.* [53] that well reproduces the resonance energies of these states. We also include 2^- state ($\ell = 0$) but neglect the d- and f-states because of the computational limit. The single particle potentials for 2^+ ($\ell = 1$) and 2^- ($\ell = 0$) states are the same as in Sec. III A. The possible configuration of $S = 1$ is not included in this analysis, following Ref. [53]. As for the discretization of the continuum states we adopt the pseudo-state method with complex-range Gaussian basis functions [40, 54]. This method was shown to reproduce resonance structure of continuum spectra of a projectile with quite small number of the discretized-continuum states. The parameters of the basis functions are ($a_1 = 1.0$, $a_n = 60.0$, $2n = 50$, $b = \pi/2$) with the same notation as in Ref. [40]. The maximum excitation energy of ${}^8\text{B}$ is taken to be 10 MeV. Then we obtain 21 discretized-continuum states for the 1^+ , 3^+ and 2^- states, and 20 for the 2^+ states, from which 420 scattering-channels are constructed. All other inputs are the same as those described in Sec. III A.

We show in Fig. 10 the result of the s- and p-state

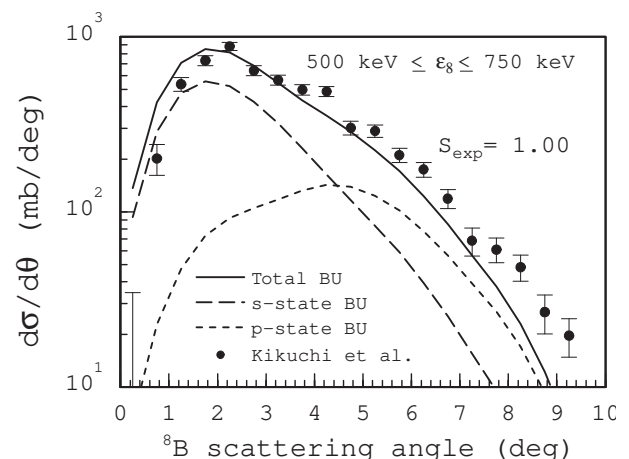


FIG. 10: The s-state (p-state) breakup cross section calculated with E-CDCC including resonance states of ${}^8\text{B}$ is shown by the dashed (dotted) line. The solid line is the sum of the two, added by the d- and f-state breakup cross sections shown in the top panel in Fig. 4.

breakup cross sections calculated with E-CDCC calculation, i.e. $L_C = 0$, by the dashed and dotted lines, respectively. We then add the d- and f-state breakup cross sections shown in the top panel in Fig. 4 incoherently and obtain the result shown by the solid line. One sees the agreement between the calculation and the experimental data for $\theta_8 > 2^\circ$ is much improved by the inclusion of the resonance states of ${}^8\text{B}$, which shows that the breakup cross section at backward angles has rather strong dependence on the details of ${}^8\text{B}$ structure. In other words, comparison between CDCC calculation and the experimental data in this angular-region can extract important information on the inner part of the ${}^8\text{B}$ wave function. In order to draw a quantitative conclusion, however, not only quantum mechanical effects on the lower partial waves but also the change in the coupling between $\ell \leq 1$ and $\ell > 1$ components by the inclusion of the resonances must be clarified. Moreover, a new filtering-table made without “s-state breakup assumption” will be necessary. In any case, effects of the resonance states of ${}^8\text{B}$ on the breakup cross section at forward angles ($\theta_8 \lesssim 2^\circ$) are very small. Therefore, we conclude that the $S_{17}(0)$ derived by CDCC calculation with no resonances of ${}^8\text{B}$ is reliable.

D. Discussion of the extracted $S_{17}(0)$

The main result of $S_{17}(0)$ in the present paper derived from ${}^{208}\text{Pb}({}^8\text{B}, p+{}^7\text{Be}){}^{208}\text{Pb}$ at 52 MeV/nucleon is $S_{17}(0) = 21.4_{-0.57}^{+0.96}$ (theo) ± 1.80 (expt) eV b. This value is significantly larger than that obtained in the previous analysis of the same experiment with the first-order perturbation theory: $S_{17}(0) = 18.9 \pm 1.8$ eV b [9]. In order to clarify the reason for the difference, we here discuss roles of nuclear interaction, E2 transitions and higher-order processes. In Fig. 11 the solid line shows the result of full CDCC that is the same as in the top panel in Fig. 4. The dashed line corresponds to the calculation without breakup-components of nuclear coupling-potentials. It should be noted that the diagonal-components of them are included in the calculation to take account of the absorption of the incident flux by the target nucleus. One sees that the dashed line perfectly agrees with the solid line below 2° and the difference between them is quite large for $\theta_8 > 3^\circ$. Thus, in the present case, the breakup processes of ${}^8\text{B}$ for $\theta_8 \leq 2^\circ$ are found to be caused purely by Coulomb coupling-potentials. It should be noted that this is true for the “smeared” cross sections; for pure theoretical results, as shown in Fig. 3, the nuclear breakup-amplitude makes the breakup cross section oscillate even at 2° .

The dotted line in Fig. 11 represents the result of one-step CDCC without nuclear breakup-components. In the one-step Coulomb calculation, all multipoles of the coupling potentials up to $\lambda = 6$ are included. Actually, effects of the coupling potentials with $\lambda \geq 3$ on the d-state breakup cross section are quite large, i.e. several

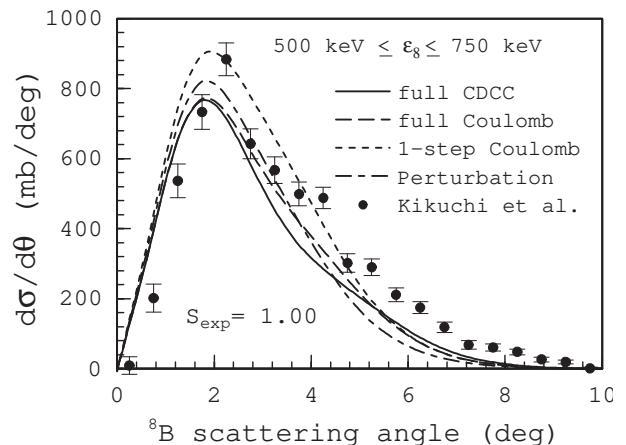


FIG. 11: The dashed (dotted) line represents the result of full CDCC (one-step CDCC) without nuclear coupling-potentials. The result of one-step CDCC including only the Coulomb E1 coupling potentials, that corresponds to the first-order perturbation theory, is shown by the dash-dotted line. The result of CDCC with nuclear and Coulomb couplings and all higher-order processes is also shown by the solid line for comparison. Note that in all calculation the diagonal (non-breakup) components of nuclear coupling-potentials are included.

tens of percent around $\theta_8 = 6^\circ$. For $\theta_8 \leq 2^\circ$, however, those on the total breakup-cross-section turned out to be less than 1%. Therefore, from now on we assume the one-step Coulomb calculation to be the one-step calculation with E1 and E2 transitions. One sees that the result of the one-step E1-E2 calculation quite overestimates the result of full-CDCC even at 1° . Thus, higher-order processes cannot be neglected to extract a reliable value of $S_{17}(0)$, which is consistent with the conclusion of Ref. [14]. If one includes only $\lambda = 1$ (E1) component of Coulomb coupling-potentials and assumes one-step transitions, the dash-dotted line in Fig. 11 is obtained. The deviation of the dash-dotted line from the solid line is somewhat smaller than that of the dotted line below about 5° . One sees from the figure that the breakup cross section of the one-step calculation with E1 transitions (dash-dotted line) is increased by the inclusion of the E2 component (dotted line) and then decreased by effects of higher-order processes (dashed line). Although the reason for this kind of “compensation” is not clear at this stage, we conclude that it is quite dangerous to evaluate the E2 contribution to the breakup cross section by an analysis with a restricted reaction mechanism.

The one-step calculation with E1 transitions can be assumed to essentially correspond to the first-order perturbation theory used in the previous analysis of the experimental data [9]. We carried out the χ^2 -fit of the result shown by the dash-dotted line to the experimental data just in the same way as in Sec. III A. Then we made the correction on $S_{17}(0)$ due to the role of the intrinsic spin of ${}^8\text{B}$; the dependence of the correction-factor \mathcal{C} on the reaction mechanisms considered was found to be negligible.

The resulting central-value of $S_{17}(0)$ is 20.2 eV b, which is quite close to the value obtained in Ref. [9], 18.9 eV b. One sees from Fig. 11 that, in the present case, first-order perturbation theory works quite well at forward angles ($\theta_8 \leq 2^\circ$) but slightly overestimates the result of CDCC. The extracted $S_{17}(0)$ with first-order perturbation is thus smaller than that obtained by CDCC; the difference between them is about 6%. Additionally, if the result of the one-step E1-E2 Coulomb calculation, the dotted line, is used in the χ^2 -fit, one obtains $S_{17}(0) = 18.8$ eV b as the central value; namely, further 6% decrease of $S_{17}(0)$ is obtained. This is consistent with the difference between the results of RIKEN [9] and MSU [13] experiments; the latter, $S_{17}(0) = 17.8_{-1.2}^{+1.4}$ eV b, was obtained with first-order perturbation theory including both E1 and (reduced) E2 components.

Thus, description of ^8B breakup process with both the E1 and E2 transitions and also with higher-order processes is a key to solve a puzzle of $S_{17}(0)$, that is, the discrepancy of the values of $S_{17}(0)$ extracted from direct p -capture reactions and indirect Coulomb-dissociation experiments. In order to clarify the role of these components in more detail, systematic analysis of ^8B breakup reactions with CDCC and the ANC method will be necessary. Analysis of parallel momentum distribution of ^7Be -fragment after breakup of ^8B is particularly important, since the role of E2 component was determined from that quantity in MSU experiment [12, 13]. Unfortunately, as mentioned above, quantitative comparison between theoretical and experimental results for ^8B breakup with high accuracy requires careful treatment of the resolution and efficiency of the measurement. Thus, at this stage, we can quantitatively extract $S_{17}(0)$ with CDCC and the ANC method only from the ^8B breakup experiment done at RIKEN.

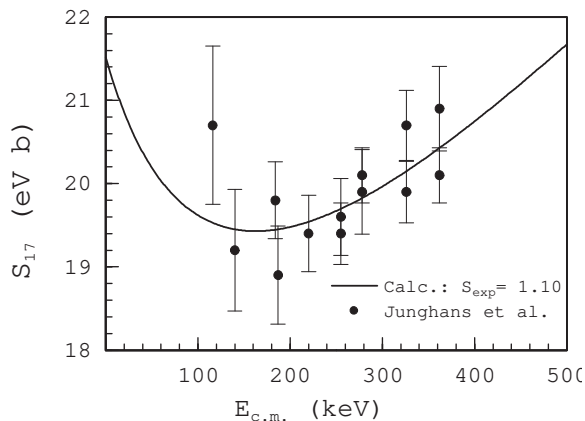


FIG. 12: The astrophysical factor S_{17} as a function of the c.m. energy of p - ^7Be . The solid line is the result of the calculation with a simple potential model, multiplied by $\mathfrak{S}_{\text{exp}} = 1.10$. The experimental data are taken from Ref. [4].

Finally, the ANC method is applied to the direct p -capture reaction $^7\text{Be}(p, \gamma)^8\text{B}$ at energies of 116–362

keV [4], with assuming a simple potential-model of ^8B . We calculated the matrix elements of the pure E1-transitions of p and ^7Be to the final state, i.e. the ground state of ^8B , including the s- and d-state components of the initial wave-function of p - ^7Be . We use the single-particle potential by Barker [46] (Esbensen and Bertsch [45]) for the initial (final) states. The intrinsic spins of p and ^7Be are explicitly included in the calculation; the configuration-mixing in the ground state of ^8B is treated just in the same way as in Sec. III B. In Fig. 12 the solid line shows the calculated S_{17} as a function of the c.m. energy $E_{\text{c.m.}}$ of p - ^7Be in the initial state. The plotted $S_{17}(E)$ has been multiplied by the spectroscopic factor $\mathfrak{S}_{\text{exp}} = 1.15$, which is the result of the χ^2 -fit using the data below 362 keV. Obviously the calculated $S_{17}(E)$ is not reliable in high-energy region, say $E_{\text{c.m.}} > 400$ keV, where the inner part of the ^8B wave function plays an important role. In contrast to that, at low energies, the ANC method works very well and a reliable value of the ANC C , or $S_{17}(0)$, can be derived from the χ^2 -fitting procedure. The resulting value of $S_{17}(0)$ is 22.2 eV b. Uncertainties of the $S_{17}(0)$ are evaluated just in the same way as in Sec. III B and found to be $+0.45/-0.28$ eV b, almost all of which is due to the ambiguity of the s-state potentials for the $S = 1$ and $S = 2$ channels of p - ^7Be . By adding the 2.3% systematic experimental error to the theoretical one in quadrature, we obtain the following result: $S_{17}(0) = 22.2_{-0.58}^{+0.68}$ eV b. This result is consistent with both the extracted $S_{17}(0)$ from ^8B dissociation in the present paper, $S_{17}(0) = 21.4_{-0.57}^{+0.96}$ (theo) ± 1.80 (expt) eV b, and the result obtained in Ref. [4], $S_{17}(0) = 22.1 \pm 0.6$ (expt) ± 0.6 (theo) eV b. It should be remarked that in the present ANC analysis the uncertainty of $S_{17}(0)$, concerning with the ambiguous p - ^7Be scattering-length, is directly evaluated, in contrast to the analysis in Ref. [4]. In that sense, our result of $S_{17}(0) = 22.2_{-0.58}^{+0.68}$ eV b obtained with the ANC method shows the validity of the result derived in Ref. [4].

IV. SUMMARY

The astrophysical factor $S_{17}(0)$ for $^7\text{Be}(p, \gamma)^8\text{B}$ is determined from $^{208}\text{Pb}(^8\text{B}, p+^7\text{Be})^{208}\text{Pb}$ at 52 MeV/nucleon measured at RIKEN, by using the asymptotic normalization coefficient (ANC) method. The peripherality, i.e. the insensitivity of the process concerned to the inner part of the ^8B wave function, is shown for the ^8B breakup process at forward angles, which is the essential condition for the ANC method to be valid. We also show the $p+^7\text{Be}+\text{A}$ three-body model is sufficient for description of the breakup process of ^8B , i.e. ^7Be can be assumed to be inert, and the breakup cross sections of ^8B are accurately calculated by means of the method of continuum-discretized coupled-channels (CDCC). In the calculation of CDCC, the scattering amplitude corresponding to large values of orbital-angular-momentum is obtained by the eikonal-CDCC method (E-CDCC) to

make efficient analysis. We have improved the formulation of E-CDCC on the treatment of the Coulomb wave function and the intrinsic spin of the projectile. The calculated angular distribution of the breakup cross section, after taking account of the resolution and efficiency for the experiment, well reproduces the measured one at forward angles and underestimates it at backward angles; the underestimation is almost removed by including resonance states of ${}^8\text{B}$.

The value of the ANC is extracted by comparing the theoretical breakup-cross-section with the experimental data at forward angles and $S_{17}(0) = 20.6$ eV b is obtained. The uncertainties of the $S_{17}(0)$ coming from the use of the ANC method and those from the ambiguity of the distorting potentials are both found to be negligible. On the contrary, uncertainties of the s-state single-particle potentials of ${}^8\text{B}$, for the $S = 1$ and $S = 2$ channels, totally bring the $+4.5\%/ -2.6\%$ error of $S_{17}(0)$. Additionally, inclusion of the intrinsic spin of ${}^8\text{B}$ is found to increase $S_{17}(0)$ by 4.0%. Thus, as the main result of the present paper, $S_{17}(0) = 21.4^{+0.96}_{-0.57}$ (theo) ± 1.80 (expt) eV b is obtained, which is consistent with the result derived from direct ${}^7\text{Be}(p, \gamma){}^8\text{B}$ measurement, $S_{17}(0) = 22.1 \pm 0.6$ (expt) ± 0.6 (theo) eV b.

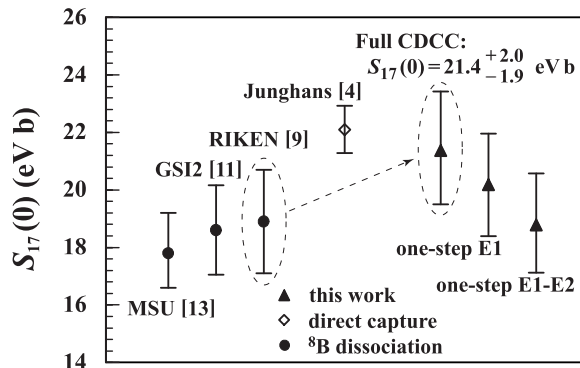


FIG. 13: The extracted $S_{17}(0)$ in the present paper are shown by triangles. The result of precise direct measurement [4] (open diamond) and those obtained from ${}^8\text{B}$ dissociation with first-order perturbation theory (closed circles) are also shown for comparison.

Although the breakup cross section at forward angles is quite well explained by the one-step Coulomb dipole (E1) transitions of ${}^8\text{B}$, this picture results in about 6% decrease of $S_{17}(0)$, namely, $S_{17}(0) = 20.2$ eV b is obtained; this value is quite close to the result of $S_{17}(0) = 18.9 \pm 1.8$ eV b determined from the same experiment by the first-order perturbation theory. The inclusion of the Coulomb quadrupole (E2) transitions in the one-step calculation is found to further decrease $S_{17}(0)$ by about 6%: $S_{17}(0) = 18.8$ eV b. Multistep processes are thus found to make $S_{17}(0)$ increase by about 12%. Consequently, in the present analysis, the E2-transition component indeed has finite effects on $S_{17}(0)$ but including it in one-step calculation leads to incorrectly low value of $S_{17}(0)$. The ANC method is also applied to direct measurement of ${}^7\text{Be}(p, \gamma){}^8\text{B}$ at energies from 116 keV to 362 keV and $S_{17}(0) = 22.2^{+0.68}_{-0.58}$ eV b is obtained, which agrees very well with the result of the recent precise measurement of $S_{17}(0)$, i.e. $S_{17}(0) = 22.1 \pm 0.6$ (expt) ± 0.6 (theo) eV b.

In conclusion, the discrepancy between the values of $S_{17}(0)$ derived from direct (p, γ) and indirect ${}^8\text{B}$ -breakup measurements is essentially removed, as shown in Fig. 13. Accurate description of the ${}^8\text{B}$ breakup process by CDCC, with E1 and E2 transitions and all higher-order processes, is of crucial importance to derive a reliable value of $S_{17}(0)$. Our main result of $S_{17}(0)$ obtained from ${}^{208}\text{Pb}({}^8\text{B}, p+{}^7\text{Be}){}^{208}\text{Pb}$ at 52 MeV/nucleon is $S_{17}(0) = 21.4^{+2.0}_{-1.9}$ eV b.

Acknowledgments

The authors would like to thank T. Motobayashi for helpful discussions and providing detailed information on the experiment. The authors also thank M. Kawai for fruitful discussions. This work has been supported in part by the Grants-in-Aid for Scientific Research of Monbukagakusyou of Japan.

-
- [1] J. N. Bahcall *et al.*, *Astrophys. J.* **555**, 990 (2001) and references therein.
 - [2] J. N. Bahcall *et al.*, *JHEP* **0108**, 014 (2001) [arXiv:hep-ph/0106258]; *JHEP* **0302**, 009 (2003) [arXiv:hep-ph/0212147].
 - [3] J. N. Bahcall, *Nucl. Phys.* **B** Proc. Suppl. **118**, 77 (2003).
 - [4] A. R. Junghans *et al.*, *Phys. Rev. C* **68**, 065803 (2003).
 - [5] P. Descouvemont and D. Baye, *Nucl. Phys.* **A567**, 341 (1994).
 - [6] P. Descouvemont, *Phys. Rev. C* **70**, 065802 (2004).
 - [7] T. Motobayashi *et al.*, *Phys. Rev. Lett.* **73**, 2680 (1994);
 - [8] T. Kikuchi *et al.*, *Phys. Lett. B* **391**, 261 (1997).
 - [9] T. Kikuchi *et al.*, *Eur. Phys. J. A* **3**, 209 (1998).
 - [10] N. Iwasa *et al.*, *Phys. Rev. Lett.* **83**, 2910 (1999).
 - [11] F. Schümann *et al.*, *Phys. Rev. Lett.* **90**, 232501 (2003).
 - [12] B. Davids *et al.*, *Phys. Rev. Lett.* **86**, 2750 (2001).
 - [13] B. Davids *et al.*, *Phys. Rev. C* **63**, 065806 (2001).
 - [14] H. Esbensen *et al.*, *Phys. Rev. Lett.* **94**, 042502 (2005).
 - [15] M. Kamimura *et al.*, *Prog. Theor. Phys. Suppl.* **89**, 1 (1986).
 - [16] N. Austern *et al.*, *Phys. Reports.* **154**, 125 (1987).
 - [17] M. Yahiro *et al.*, *Prog. Theor. Phys.* **67**, 1467 (1982).
 - [18] M. Yahiro *et al.*, *Phys. Lett.* **141B**, 19 (1984).
 - [19] Y. Sakuragi and M. Kamimura, *Phys. Lett.* **149B**, 307

- (1984) .
- [20] Y. Sakuragi, Phys. Rev. C **35**, 2161 (1987).
- [21] Y. Sakuragi *et al.*, Phys. Lett. **B205**, 204 (1988); Nucl. Phys. **A480**, 361 (1988).
- [22] Y. Iseri *et al.*, Nucl. Phys. **A490**, 383 (1988).
- [23] Y. Hirabayashi and Y. Sakuragi, Phys. Rev. Lett. **69**, 1892 (1992).
- [24] J. A. Tostevin *et al.*, Phys. Rev. C **66**, 024607 (2002); A. M. Moro, R. Crespo, F. Nunes and I. J. Thompson, Phys. Rev. C **66**, 024612 (2002) and references therein.
- [25] K. Ogata, M. Yahiro, Y. Iseri and M. Kamimura, Phys. Rev. C **67**, 011602(R) (2003).
- [26] J. A. Tostevin, F. M. Nunes and I. J. Thompson, Phys. Rev. C **63**, 024617 (2001).
- [27] J. Mortimer, I. J. Thompson and J. A. Tostevin, Phys. Rev. C **65**, 064619 (2002).
- [28] K. Ogata *et al.*, Nucl. Phys. **A 738c**, 421 (2004).
- [29] A. M. Mukhamedzhanov and N. K. Timofeyuk, Yad. Fiz. **51**, 679 (1990) [Sov. J. Nucl. Phys. **51**, 431 (1990)].
- [30] H. M. Xu, C. A. Gagliardi, R. E. Tribble, A. M. Mukhamedzhanov and N. K. Timofeyuk, Phys. Rev. Lett. **73**, 2027 (1994).
- [31] J. von Schwarzenberg *et al.*, Phys. Rev. C **53**, R2598 (1996); J. J. Kolata *et al.*, Phys. Rev. C **63**, 024616 (2001).
- [32] D. C.-Gil *et al.*, Phys. Lett. B **529**, 36 (2002).
- [33] K. Ogata, M. Yahiro, Y. Iseri, T. Matsumoto and M. Kamimura, Phys. Rev. C **68**, 064609 (2003).
- [34] D. Baye, Phys. Rev. C **62**, 065803 (2000).
- [35] A. Azhari *et al.*, Phys. Rev. Lett. **82**, 3960 (1999).
- [36] A. Azhari *et al.*, Phys. Rev. C **60**, 055803 (1999).
- [37] Y. Iseri *et al.*, Prog. Theor. Phys. Suppl. **89**, 84 (1986).
- [38] N. Austern, M. Yahiro and M. Kawai, Phys. Rev. Lett. **63**, 2649(1989); N. Austern, M. Kawai and M. Yahiro, Phys. Rev. C **53**, 314 (1996).
- [39] M. Yahiro and M. Kamimura, Prog. Theor. Phys. **65**, 2046 (1981); **65**, 2051 (1981).
- [40] T. Matsumoto *et al.*, Phys. Rev. C **68**, 064607 (2003).
- [41] A. M. Moro *et al.*, Phys. Rev. C **65**, 011602(R) (2001).
- [42] R. Y. Rasoanaivo and G. H. Rawitscher, Phys. Rev. C **39**, 1709 (1989).
- [43] M. Kawai, private communication (2003).
- [44] See, for example, Y. Watanabe *et al.*, Phys. Rev. C **59**, 2136 (1999).
- [45] H. Esbensen and G. F. Bertsch, Nucl. Phys. **A600**, 66 (1996).
- [46] F. C. Barker, Aust. J. Phys. **33**, 177 (1980).
- [47] C. Angulo *et al.*, Nucl. Phys. **A716**, 211 (2003).
- [48] A. J. Koning and J. P. Delaroche, Nucl. Phys. **A713**, 231 (2003).
- [49] J. Cook, Nucl. Phys. **A388**, 153 (1982).
- [50] T. Motobayashi, private communication (2004).
- [51] K. H. Kim, M. H. Park and B. T. Kim, Phys. Rev. C **35**, 363 (1987).
- [52] I. Tanihata *et al.*, Phys. Rev. Lett. **55**, 2676 (1985).
- [53] S. Typel *et al.*, Nucl. Phys. **A613**, 147 (1997).
- [54] E. Hiyama *et al.*, Progress in Particle and Nuclear Physics **51**, 223 (2003).